ER-7588

CORROSION FATIGUE BEHAVIOR OF 4340 STEEL ABOVE K_{ISCC}

TECHNICAL REPORT

Prepared for
Office of Naval Research
Contract N00014-69-C-0286

JULY, 1972

By
C. S. KORTOVICH
E. A. STEIGERWALD

TRW
EQUIPMENT
MATERIALS TECHNOLOGY

49

ER 7588

Technical Report

CORROSION FATIGUE BEHAVIOR OF 4340 STEEL ABOVE K_{Iscc}

Prepared for

Office of Naval Research
Contract N00014-69-C-0286

July 1972

By

C. S. Kortovich
and
E. A. Steigerwald

TRW Inc.
TRW Equipment
Materials Technology
Cleveland, Ohio 44117

FOREWORD

The work described in this report was performed under sponsorship of the Office of Naval Research, Contract N00014-69-C-0286 with Dr. P. Clarkin acting as program manager for the Navy. The effort on this contract during the first year dealt with "A Critical Evaluation of Hydrogen Embrittlement Mechanisms" and a paper on this subject was published in Metallurgical Transactions, Volume 1, December 1970. The second year's effort, "A Comparison of Hydrogen Embrittlement and Stress Corrosion Cracking in High Strength Steels," will be published in 1972 in the Journal of Fracture Mechanics. Work conducted during the third year of this contract, covered in this report, involved a study of the corrosion fatigue behavior of AISI 4340 steel in aqueous media above K_{Iscc}. Attempts were made in this study to superimpose the fatigue crack growth behavior in an inert atmosphere onto the environmental contribution determined from delayed failure tests and thereby to predict the corrosion fatigue behavior in aqueous media.

This report has been assigned TRW Equipment Number ER-7508 and the data are reported in laboratory notebook No. 481.

ABSTRACT

The purpose of this program was to study the corrosion fatigue behavior of AISI 4340 in distilled water above K_{Iscc}. The results obtained by superimposing fatigue crack growth behavior determined in an inert argon atmosphere onto the environmental contribution determined from sustained load stress corrosion tests indicated that a modification of the Wei-Landes model was required to improve the predictability of the corrosion fatigue behavior. This indicated that the stress corrosion contribution to corrosion fatigue is a complex function of K_I, particularly at load cycles which are close to K_{Iscc}.

Activation energies for crack growth in stress corrosion and corrosion fatigue indicate that the kinetics are controlled by the metal-environment reaction occurring at the crack surface.

TABLE OF CONTENTS

I - INTRODUCTION AND BACKGROUND

The reversible hydrogen embrittlement of high strength steels has been a critical design problem and a theoretical challenge for several decades. The phenomenological and mechanistic aspects of this problem were initially investigated utilizing a "closed" system, wherein the hydrogen was introduced prior to the application of a load (1-6). Under these conditions the delayed failure behavior in notched specimens consisted of the following characteristics: (1) an incubation time which preceded crack initiation, (2) a period of slow crack growth which was usually discontinuous in nature, and (3) a lower critical stress below which failures were not observed in times of engineering significance.

Many of the phenomenological aspects characteristic of failure in hydrogen charged specimens have been observed in the delayed failure of high strength steels in aqueous media (7-11). Interest in this stress corrosion failure of high strength steels has increased during recent years because: (1) steels are now used at higher strength levels in several classes of vehicles, including merchant ships, (2) the higher strength steels are more susceptible to stress corrosion failure than the lower strength steels of the same composition, and (3) the consequence of a stress corrosion crack in a high strength steel can be the initiation of catastrophic brittle failure. Studies were conducted at TRW to compare the known behavior of hydrogen embrittled high-strength steel to the characteristics of environmentally induced stress corrosion failure where hydrogen is continuously generated at the specimen surface (12). Results indicated that the incubation time for the initiation of crack growth was related to either a critical amount of dissolution or permeation of a barrier film at the crack tip. The incubation time was not completely reversible with respect to applied stress and diffusivity measurements indicated that the process kinetics were independent of hydrogen diffusion. These incubation time studies and the diffusivity measurements were consistent with the conclusion that the failure process is controlled by the hydrogen generating metal-environment reaction.

In view of the fact that metal-environmental reaction kinetics govern the time dependent aspects of stress corrosion, it is believed that any system perturbation such as cyclic loading which can alter this surface reaction could also change the embrittlement kinetics. Studies have shown that the joint action of environment and cyclic loading (corrosion fatigue) can be extremely degrading to the load carrying capability of a material (13). Corrosion fatigue action has produced material damage for almost any combination of applied stress level, material, heat treatment and corrosive agent.

The background data on both hydrogen embrittlement and stress corrosion represent a basis for studying the mechanism that governs the corrosion fatigue phenomenon. Historically, the problem of environment enhanced crack growth under sustained loads (stress corrosion cracking) and in fatigue (corrosion fatigue) have been treated as separate problems. In a recent review Wei (13) suggested that the mechanism for moisture and hydrogen enhanced subcritical-crack growth in high strength steels under sustained load and in fatigue may be the same. This suggestion was based on the fact that nearly all of the effects of water vapor, hydrogen and oxygen on subcritical-crack growth under sustained loads reported by Johnson and Willner (14) and Hancock and Johnson (15) were reproduced for fatigue (16-18). Fractographic evidence showing that the predominant paths of fracture in a 18Ni-250 maraging steel tested in dehumidified hydrogen at room temperature under sustained load and in fatigue were the same, lends further support to this viewpoint (19). The corresponding crack growth data (18,20), Figure 1, show that the rates of fatigue-crack growth in hydrogen depend strongly on the test frequency, whereas the rates of fatigue-crack growth in argon are nearly independent of the test frequency; and that the form of the fatigue-crack growth rate versus $K_{I\max}$ (where $K_{I\max}$ is the maximum value of the crack-tip stress intensity factor during one fatigue cycle), is quite similar to the growth rate versus K_I curves under sustained loads.

These results suggest that the observed frequency effect is the result of environment-enhanced crack growth rather than a reflection of the rate sensitivity of the material. In view of this, a simple superposition principle has been proposed to predict corrosion fatigue rates (19). Fatigue crack growth in high strength steels in an aggressive environment is considered to be composed of two components - a mechanical component and an environmental component. The rate of fatigue-crack growth, to a first order approximation, is simply considered as equal to the algebraic sum of these two components. The mechanical component represents the rate of fatigue-crack growth in the absence of an external environment and is determined experimentally by testing in an inert environment or in vacuum. The environmental component is determined from experimental crack-growth data under sustained loading in the appropriate envrionment and the fatigue-load profile, which would incorporate both the loading variables, (mean load, load amplitude, and wave form), and frequency.

Above $K_{I\,scc}$ (the maximum stress-intensity factor at the crack tip which will not produce failure in times of engineering significance) a distinct increase in slow crack growth rate occurs under cyclic loading conditions, and the stress corrosion and fatigue cracking mechanisms are assumed to proceed independently without synergistic effects. The regions where the specific contributions of fatigue and stress corrosion are operative are shown in Figure 2 with the contributions of the stress corrosion environment being integrated in the load-time history of the fatigue cycle. K_{Ic} is the plane-strain fracture toughness of the material and K_{th} is the stress intensity factor below which cracks do not proporate.

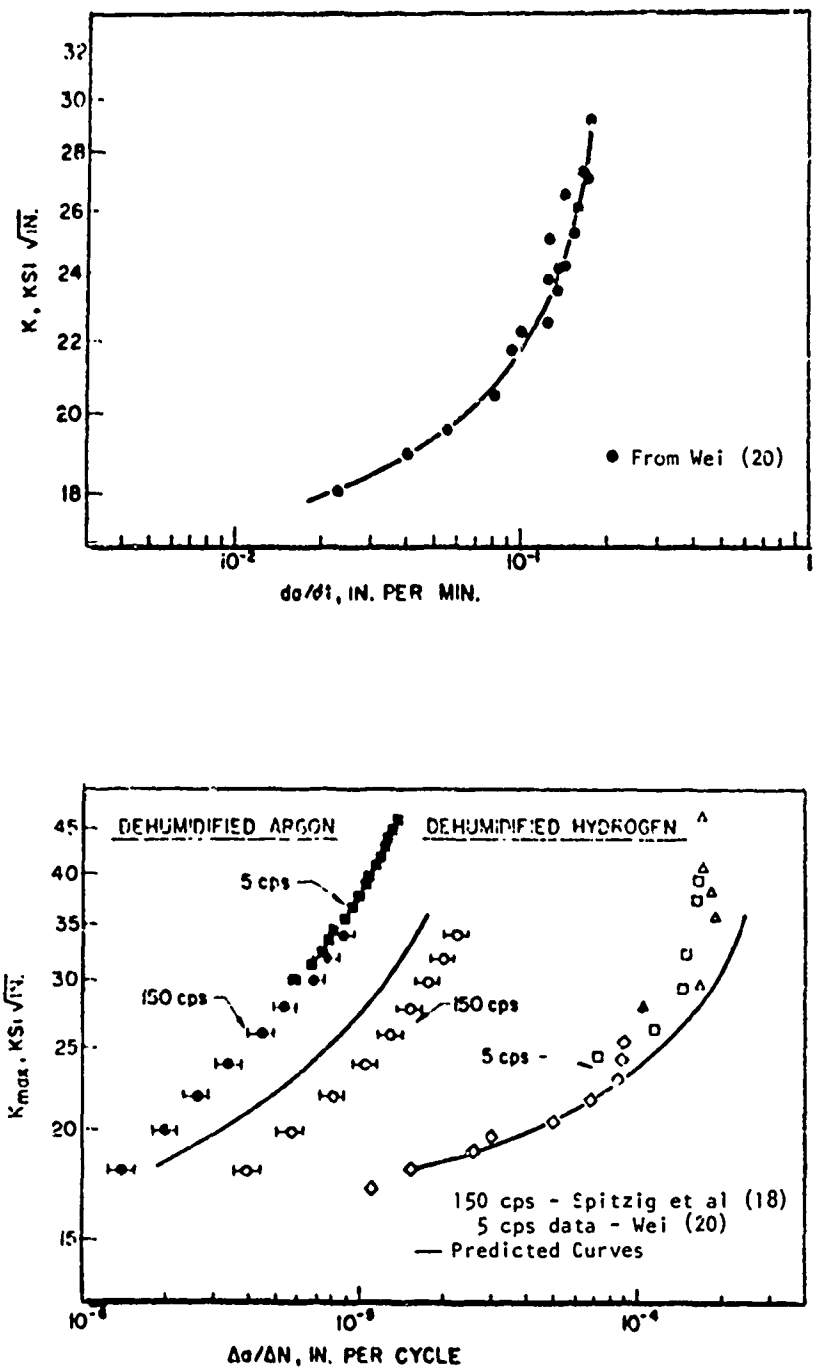

Figure 1. Stress corrosion and corrosion fatigue crack growth behavior characteristic of high strength steel. (18,20)

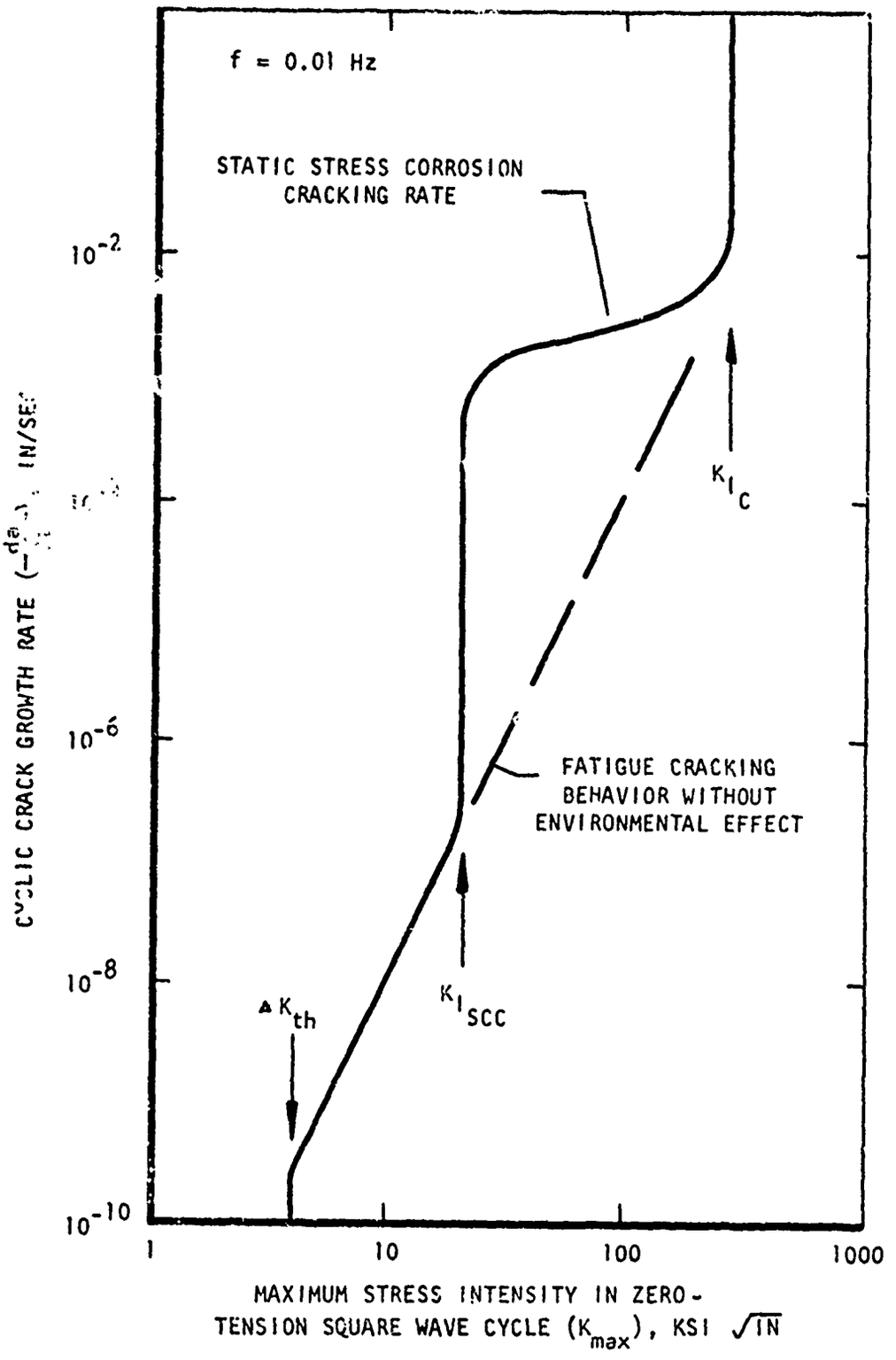

Figure 2. Schematic illustration of contribution of environment to cyclically induced crack growth.

The linear superposition principle of Wei and Landes (19) is presented in equation form as:

$$\left[\frac{da}{dn}\right]_c = \left[\frac{da}{dn}\right]_s + \left[\frac{da}{dn}\right]_R$$

where $[da/dn]_c$ is the crack growth rate under the corrosion fatigue condition (c), the stress corrosion condition (s), and the fatigue condition ($R = K_{Imin}/K_{Imax}$).

The environmental contribution is expressed in the form:

$$\left[\frac{da}{dn}\right]_s = \gamma\int\frac{da}{dn}dt$$

where the integral is taken over one period of loading (γ) and the crack growth rate in the integrand is a function of stress intensity (K_I) which varies with time.

Although the behavior of corrosion fatigue from the standpoint of crack growth rate, frequency and mean load can be qualitatively predicted above K_{Iscc} by the superposition principle, there are still many apparent anomalies in both the utilization and interpretation of the data. For example, crack growth behavior under static load can accelerate as a function of applied K_I level until a constant value is reached. The functional dependence of da/dt in this case can be relatively complex, and the calculated crack growth can be considerably greater than that observed under corrosion fatigue conditions. In addition, recent work has indicated that incubation time effects can be relatively long (approaching 5000 hours) in certain steels when tested at K_I levels in the vicinity of the apparent K_{Iscc} (21). No provision for this behavior is available in the superposition model. Also, the model predicts that the environmental contribution towards corrosion fatigue crack growth rate becomes operative as soon as the applied stress intensity exceeds K_{Iscc}. This may not necessarily be correct, particularly if there are residual compressive stresses remaining at the crack tip which actually lower the applied stress intensity.

Although certain limitations are apparent in the applicability of the superposition method for the analysis of corrosion fatigue phenomena, the method does provide a useful basis for the development of a meaningful cumulative damage rule for estimating the serviceable lives of engineering structures. The ability to predict the rates of fatigue crack growth in an agressive environment, directly from experimental data on fatigue-crack growth in an inert environment and those for sustained-load crack growth in the appropriate environment would drastically reduce the amount of testing required Further development and experimental verification of this method is needed

The purpose of this study was to couple the basic concept of the hydrogen embrittlement model and the prediction capability for delayed failure in aqueous environments to develop a model for explaining environmentally accelerated fatigue crack growth. The experimental approach involved a determination of the environmentally-induced delayed failure crack growth (da/dt) of 4340 steel exposed to distilled water and a static load, and the acceleration of fatigue crack growth rate due to environment at two different frequencies, a range of applied stress levels, and three different test temperatures. These results were analyzed to provide an indication of the factors controlling corrosion fatigue and to determine whether a superposition model could predict corrosion fatigue kinetics.

II - MATERIALS AND PROCEDURES

A commercial heat of 0.750" thick air melted SAE-AISI 4340 steel with the following composition was used for the program:

Composition of 4340 Steei (w/o)

Source and Heat No.	C	Si	Mn	Cr	Mo	Ni	P	S	Cu	Fe
Earle M Jorgensen Heat 50016	0.42	0.31	0.72	0.85	0.22	1.84	0.010	0.010	0.11	Balance

The tests were conducted on precracked compact K_{Ic} plate specimens 0.5" thick having the configuration shown in Figure 3. The specimens were heat treated prior to finish machining according to the following sequence:

1. Normalize 15 minutes, salt bath at 1700°F, air cool.
2. Austenitize 30 minutes, salt bath at 1550°F, oil quench.
3. Temper in air, 1 hour plus 1 hour at 750°F, air cool.

The average mechanical properties produced by these heat treatments are summarized in Table 1.

Table 1

Room Temperature Mechanical Properties of 4340 Steel, 750°F Temperature

Ultimate Tensile Strength (ksi)	225.2
0.2% Offset Yield Strength (ksi)	212.1
% Elongation	11.2
% Reduction Area	42.4

To facilitate the formation of a fatigue precrack, an EDM slot was placed at the root of the machined notch 0.050" deep and 0.010" thick. Precracking was then performed after heat treatment on an SF-1U Sonntag fatigue machine at stresses which provided the desired crack length (0.6") in 140,000 to 180,000 cycles. After precracking, all specimens were cleaned with acetone and stored in a dissicator until tested.

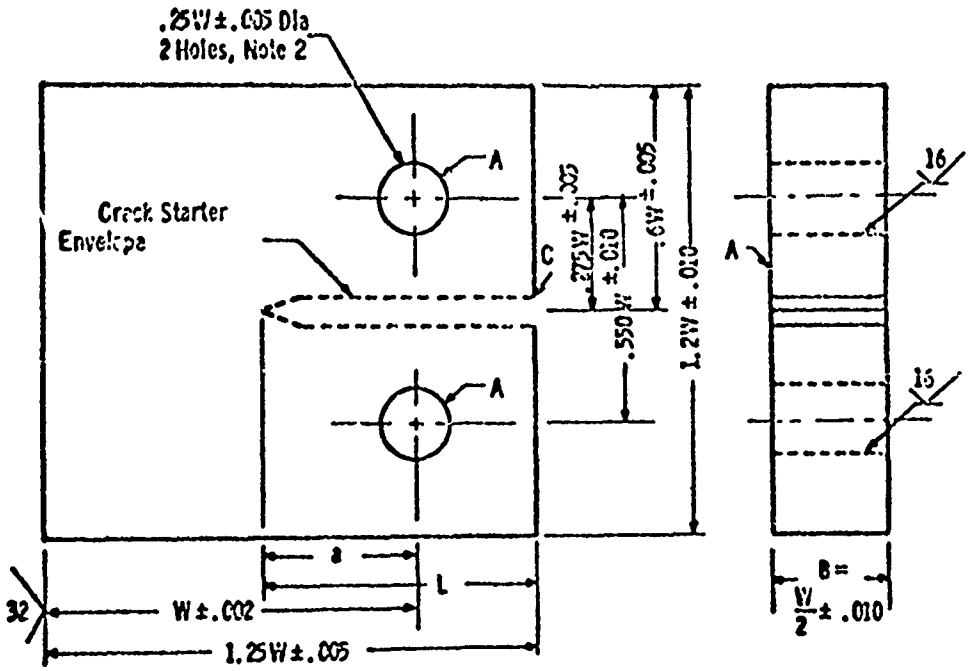

W = 1.0"
A = 0.35"
B = 0.50"

Figure 3. Precracked compact K_{Ic} plate specimen.

The sustained load delayed failure tests of the plate specimens were conducted on self-leveling lever-loaded Satec creep rupture machines in distilled water at 32°F, 70°F, and 212°F. The environment was applied immediately before the application of the load by attaching a plexiglass container to the bottom pull bar of the creep rupture rack. The bottom threaded grips as well as the specimen area in the vicinity of the precrack were exposed to the environment, Figure 4A.

A cantilever beam clip gauge was designed for these single-edge notch specimens, Figure 4B, in which the compliance was measured by strain gauges attached to the upper and lower faces of the clip gauge beam, the strain bridge output being fed into a single pen recorder. Crack growth characteristics were measured by recording changes in the specimen compliance. After conversion from compliance to crack length, slopes were obtained at various values of crack length and plotted versus the instantaneous stress intensity. In addition to the crack growth rates, the K_{Iscc} for the various temperatures were determined and utilized as a basis for applying the superposition principle to predict the corrosion fatigue phenomenon.

Corrosion fatigue tests were conducted with the same compact K_{Ic} specimens used in the sustained load tests (see Figure 4). Load control testing was performed on an Instron tensile testing machine using two different ΔK levels and frequencies of 2.4 and 24 cpm. Crack growth kinetics were determined with a compliance gauge for test conditions involving an inert atmosphere of dehumidified argon at room temperature and distilled water at 32°F, room temperature, and 212°F. The dehumidified argon atmosphere was obtained by passing the inert gas through a column of magnesium perchlorate before entering the sealed plexiglass environmental test chamber.

Barsom (22) has observed that environmental effects in corrosion fatigue near or below K_{Iscc} do not occur during the constant-load portion of each load excursion. Therefore, a varying load-time profile was established to examine this phenomenon. In Figure 5 a typical saw-tooth load-time profile is shown from an Instron testing machine utilized in this program.

The Wei-Landes analysis (19) was utilized to predict the slow crack growth rate in corrosion fatigue near and above K_{Iscc}.

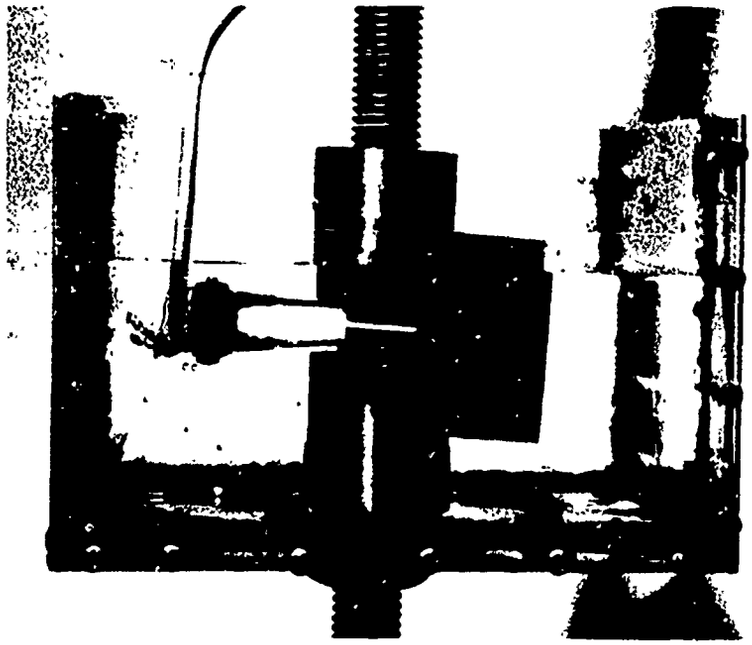

A. Compact K_{Ic} plate specimen in distilled water showing attached compliance gauge.

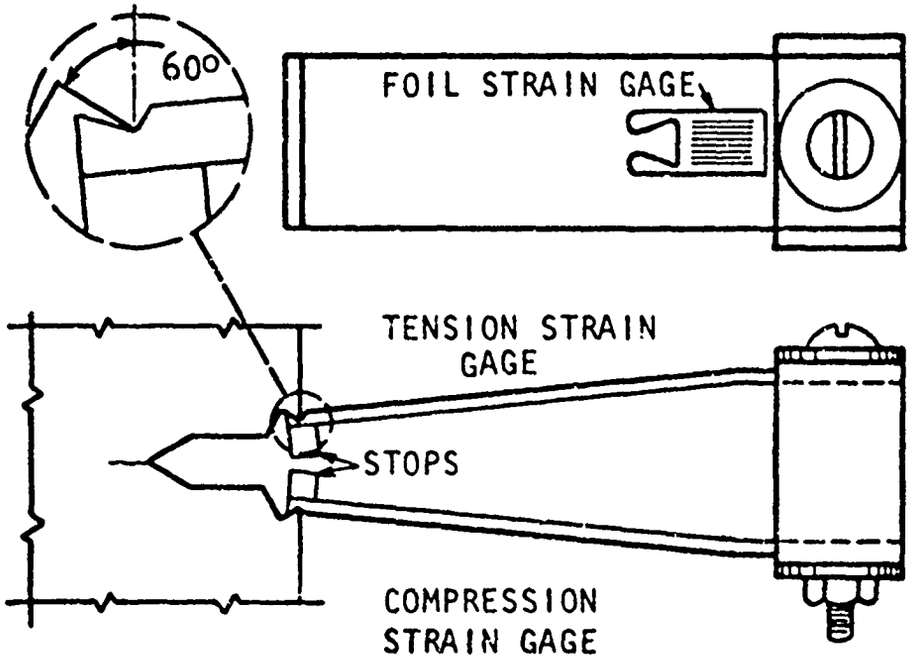

B. Schematic illustration of compliance gauge.

Figure 4. Photograph and schematic illustration of compliance gauge mounted on compact K_{Ic} plate specimen.

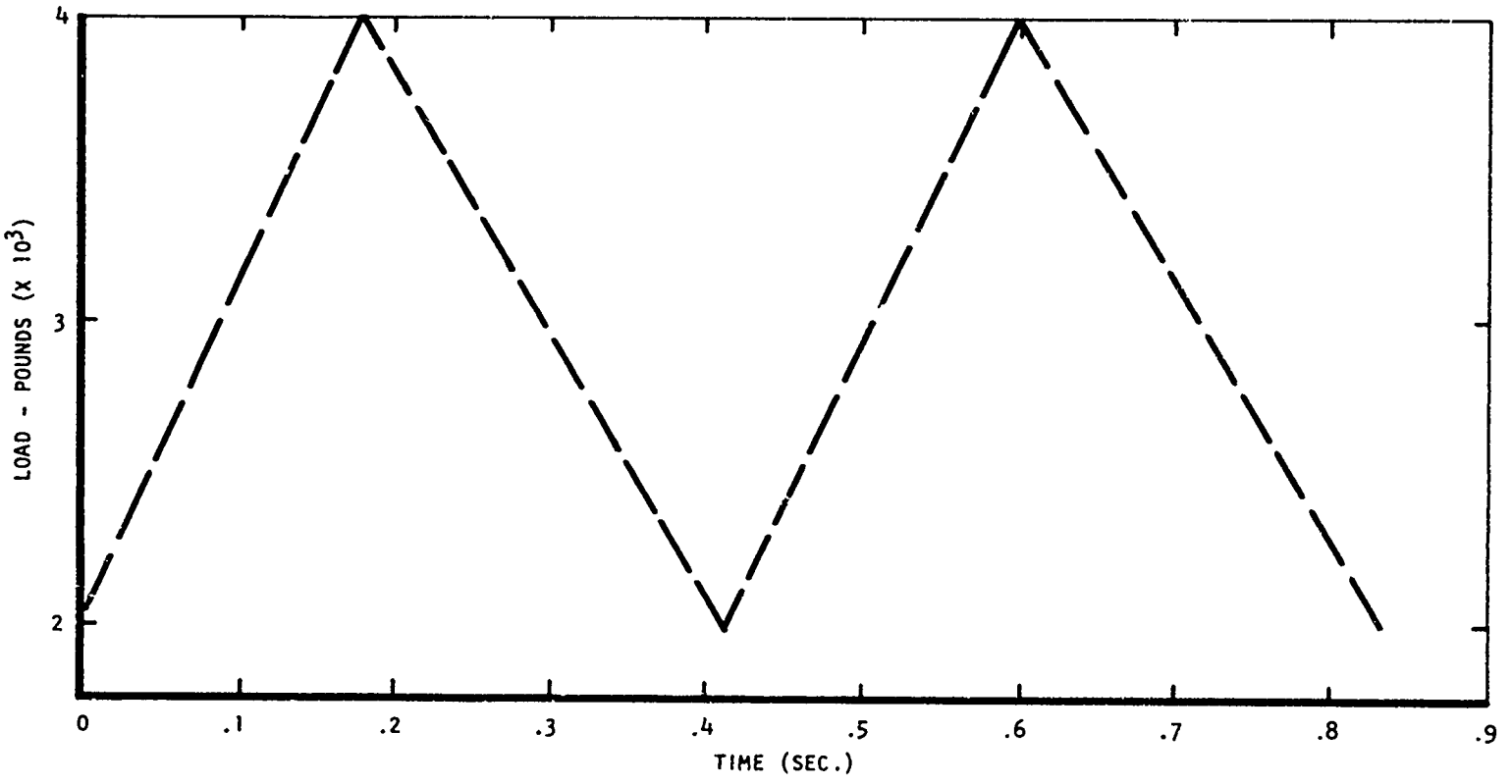

Figure 5. Schematic illustration of the type saw-tooth load-time profile used in corrosion fatigue portion of program. Load cycles between 2000 and 4000 pounds and a frequency of 2.4 cpm.

III - RESULTS AND DISCUSSION

The overall objective of this program was to develop a mechanism to explain the corrosion fatigue phenemenon in high strength steels exposed to aqueous environments. At present the current embrittlement explanations are rather broad models which usually apply only to specific steels. In this study the influence of the primary test variables on environmentally induced delayed failure under static load and cyclic load were determined to evaluate whether or not a superposition model is applicable to predict corrosion fatigue crack growth rates and what modifications might be required.

A. Environmentally-Induced Failure Under Static Load

1. Failure Characteristics

In order to serve as a basis for studying environmental acceleration in fatigue, sustained load tests were conducted at 32°F, 70°F, and 212°F. The delayed failure curves are shown in Figures 6, 7, and 8. The essential characteristic of this stress corrosion delayed failure behavior was similar to those of hydrogenated high strength steels in that (1) cracking proceeded discontinuously until a critical length was attained followed by rapid failure, (2) failure time varied only slightly with applied stress intensity, and (3) a lower critical stress (K_{Iscc}) was obtained below which delayed failure was not observed.

In general, the severity of environmental embrittlement in this high strength steel was quite temperature dependent. At room temperature, failures were observed within 80 minutes at stress intensities which were approximately 50-75% of the notch value in air. At 212°F failures were observed at 50 minutes at stress intensities as low as 33% of the notch value, while at 32°F, failures at 50-75% of the notch stress intensity level were not observed until over 200 minutes.

2. Effect on Lower Critical Limit (K_{Iscc})

In addition to the effect upon failure times, environment temperature also affected the lower critical stress (K_{Iscc}) in an interesting manner. As indicated in Figure 9A, it has been established that K_{Iscc} at room temperature decreases as yield strength increases for a variety of high strength steels, including 4340 (23). Data obtained from the present program, Figure 9B, indicate that K_{Iscc} decreases with increasing temperature, but when compared to the yield strengths at test temperature (handbook values (24)), show an increase with yield strength. This apparent anomalous behavior with respect to yield strength can be explained in terms of the stress corrosion cracking mechanism which describes the primary cause of environmental embrittlement to be hydrogen produced by the corrosion process at the material surface (7).

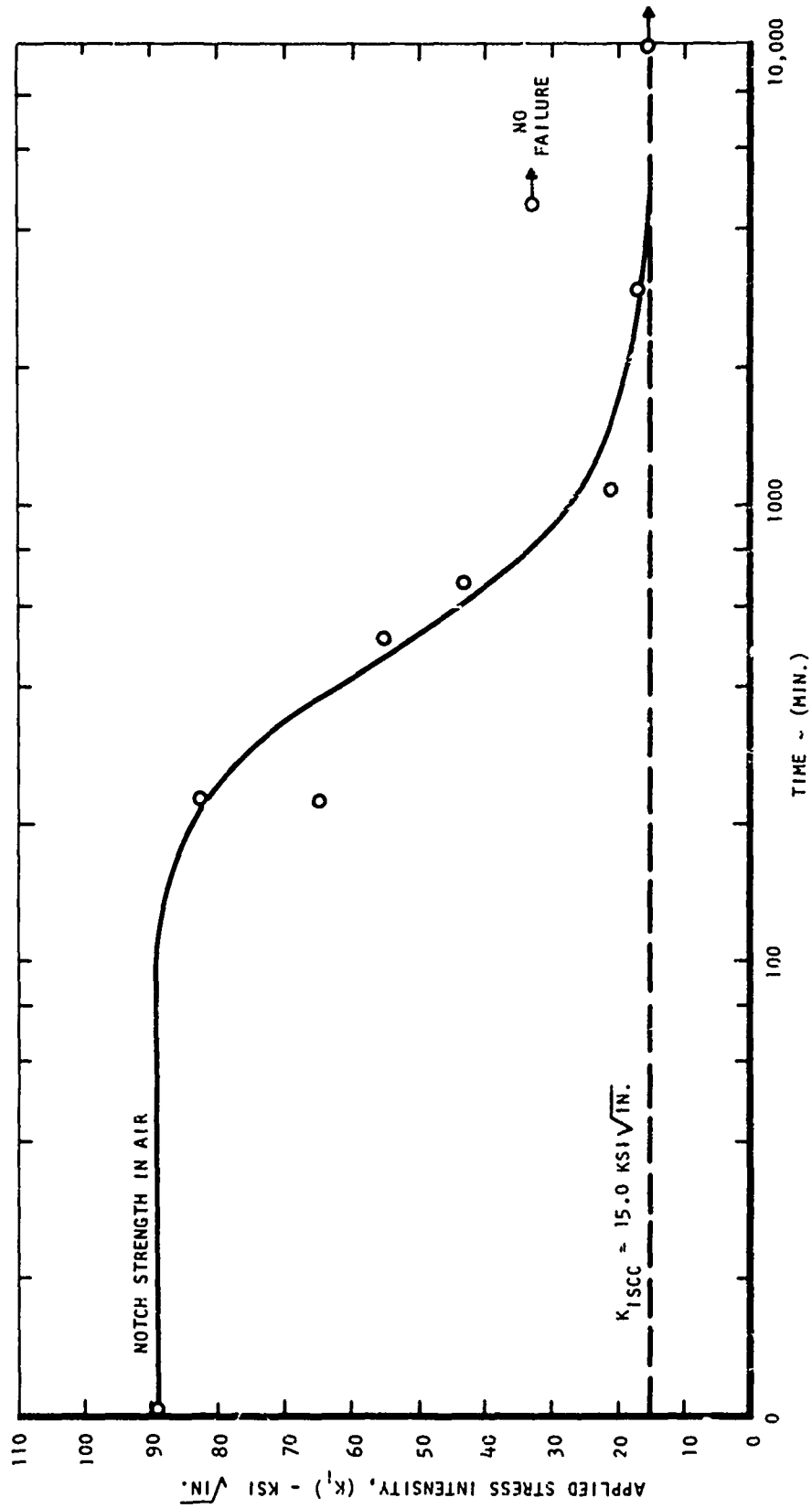

Figure 6. Delayed failure curve for 4340 steel, 750°F temper, exposed to distilled water environment at 32°F, precracked specimens.

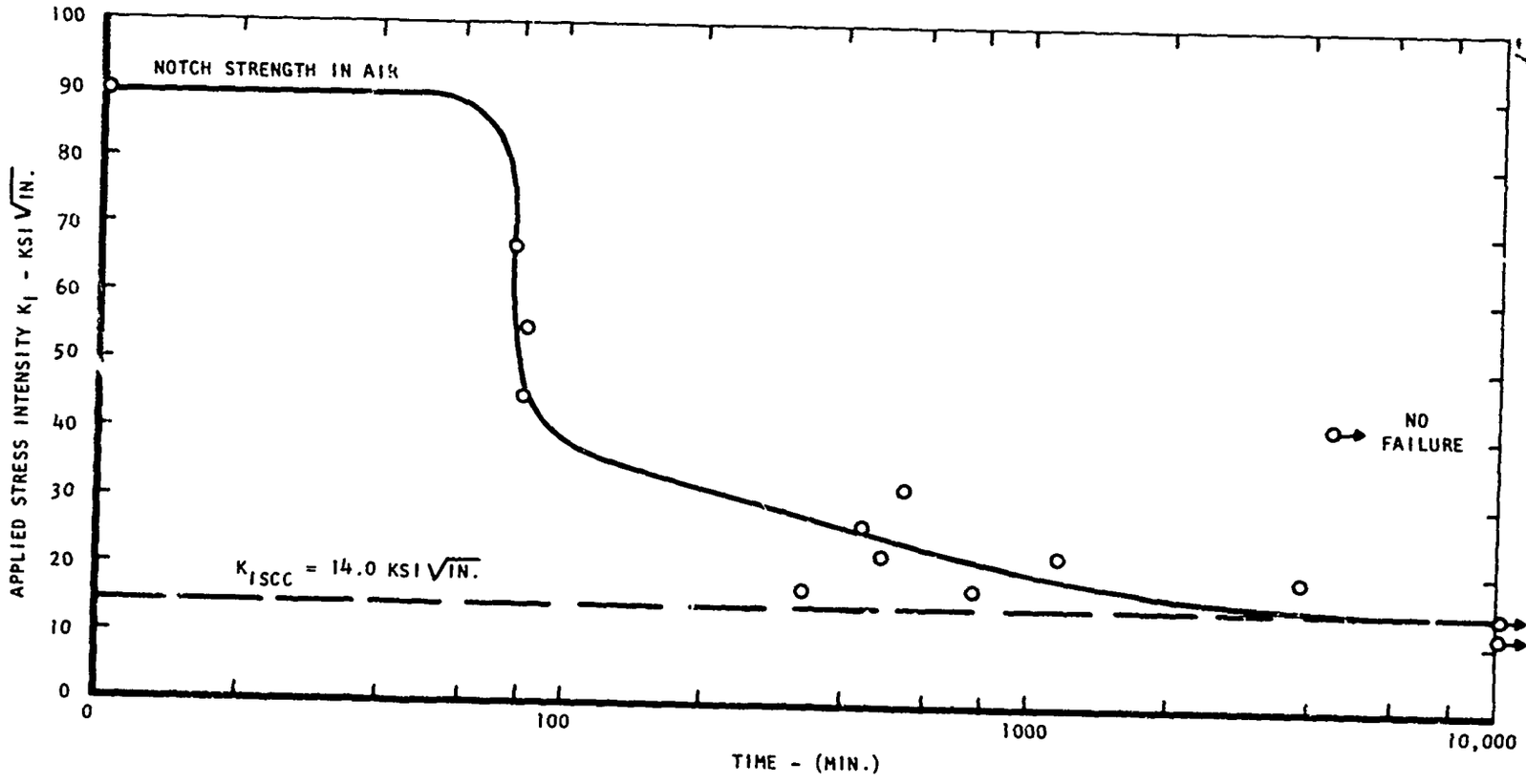

Figure 7. Delayed failure curve for 4340 steel, 750°F temper, exposed to distilled water environment at 70°F, precracked specimens.

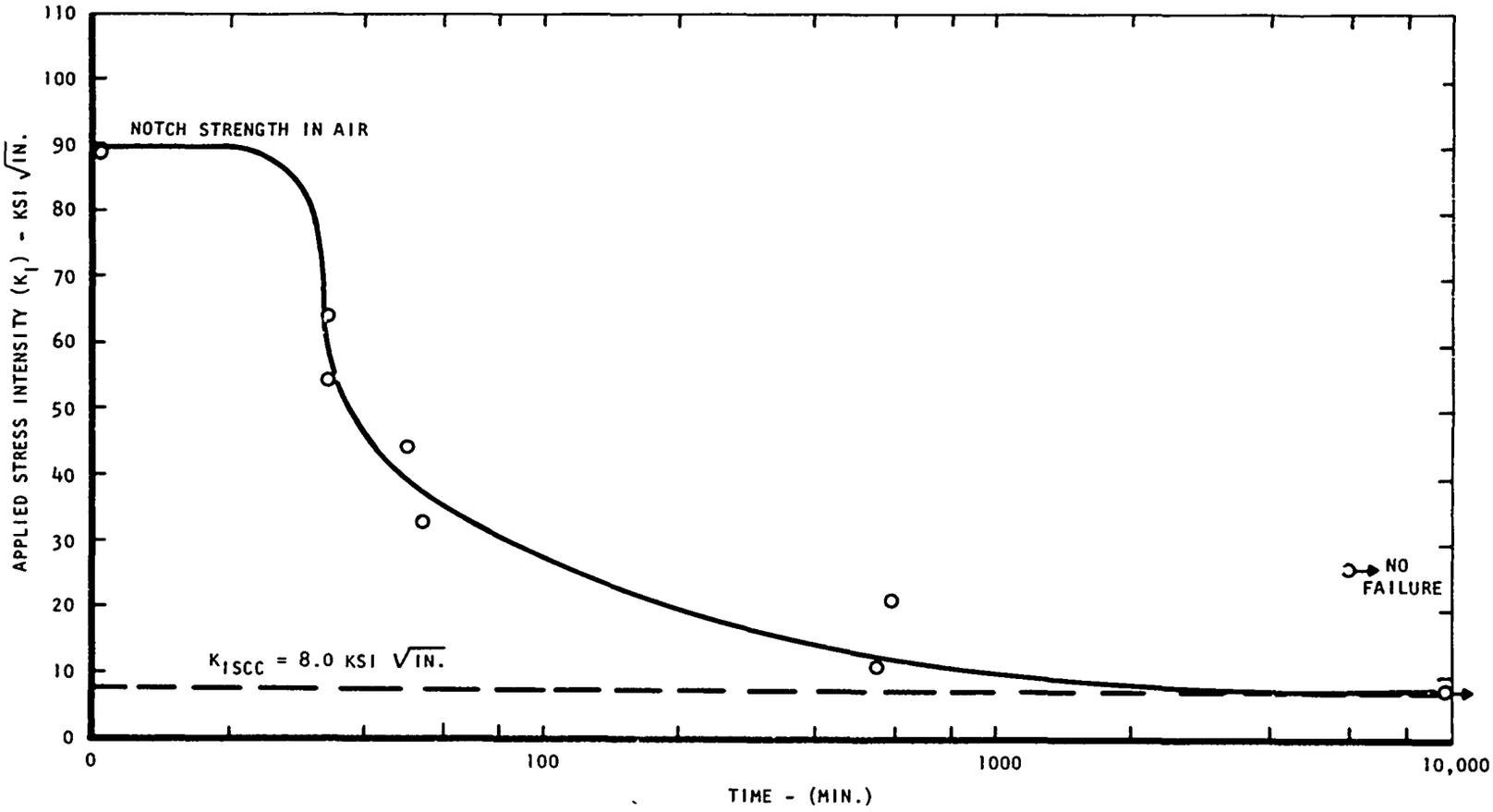

Figure 8. Delayed failure curve for 4340 steel, 750°F temper, exposed to distilled water environment at 212°F, precracked specimens.

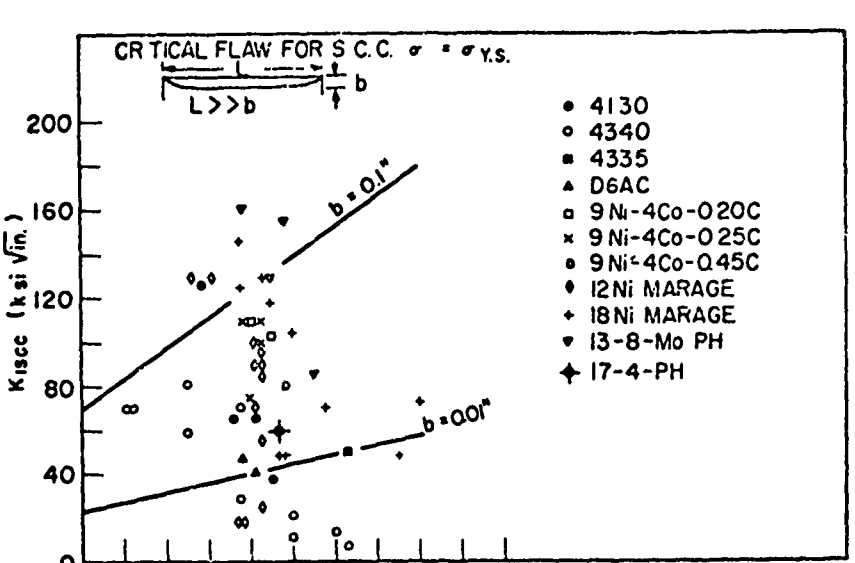

A. K_{Iscc} for some commercial steels in salt water, shown as a function of yield strength. (Data of Sandoz and Newbegin, NRL.) (23)

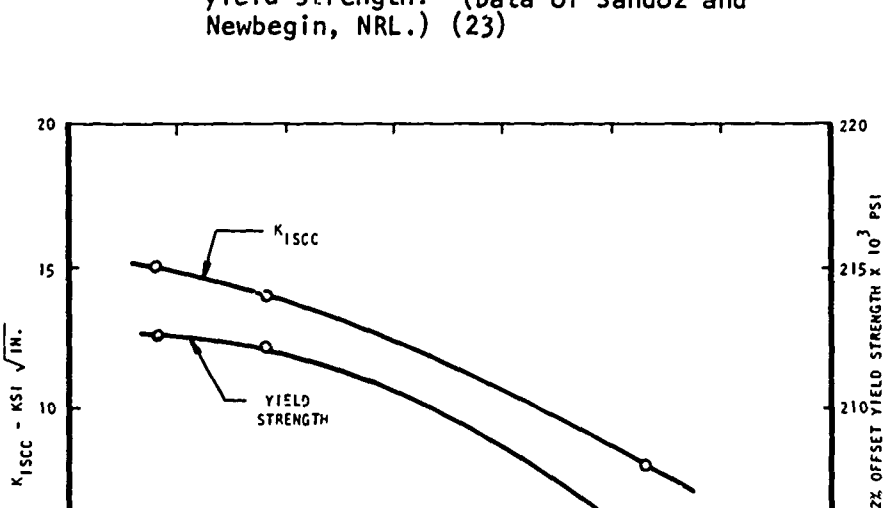

B. K_{Iscc} and 0.2% offset yield strength versus test temperature

Figure 9. Effect of yield strength and test temperature on K_{Iscc} of 4340 and other selected materials.

If it can be assumed that the kinetics of the corrosion process are temperature dependent, at constant temperature the delayed failure and K_{Iscc} characteristics would depend upon the structure sensitive properties of the material, i.e., the yield strength, Figure 9A. As temperature varies, the corrosion reaction is either accelerated or inhibited, thereby becoming the rate controlling factor. For example, at 212°F, although the yield strength for 4340 has decreased, the corrosion rate has increased at the surface, promoting more severe embrittlement than at room temperature, even though the yield strength would be greater, Figure 9B.

3. Crack Growth Behavior

In studying crack growth under stress corrosion conditions, it has been generally assumed that there is a one-to-one correspondence between crack growth rate and the mechanical crack driving force characterized by K_I. This certainly exists for the case of steady-state crack growth, but it does not necessarily preclude the occurrence of a number of nonsteady-state phenomena. The crack growth process has been shown to be divided into six stages (21):

a. crack extension on rising load

b. initial transient crack growth

c. incubation period

d. crack acceleration

e. steady-state crack growth

f. crack growth instability

In order to apply the superposition principle to corrosion fatigue, the environmental contribution must be considered with respect to these stages because utilization of this principle assumes that crack growth occurs under steady-state conditions. The following discussion is included because of the implications of nonsteady-state crack growth on the predictability of corrosion fatigue. The occurrence of crack extension on loading, followed by transient growth, has been observed by Li et al (16), Barsom (21), and Landes and Wei (21). This behavior is illustrated schematically in Figure 10A. Following the initial transient growth, the crack appears to stop growing, or enter an incubation period, before accelerating again to some steady-state rate of growth appropriate to the prevailing K_I. Landes and Wei showed that this nonsteady-state growth period is a function of K_{Ii}, the initial stress intensity, Figure 10B. The existence of an incubation period for precracked specimens has been demonstrated by Benjamin and Steigerwald (25) on AISI 4340 steel tested in water, and was shown to be affected by prior history. As shown by Wei, Noval, and Williams (21) for a highly alloyed 180 ksi yield-strength steel tested in sea water, the incubation period can be quite long in certain alloy systems.

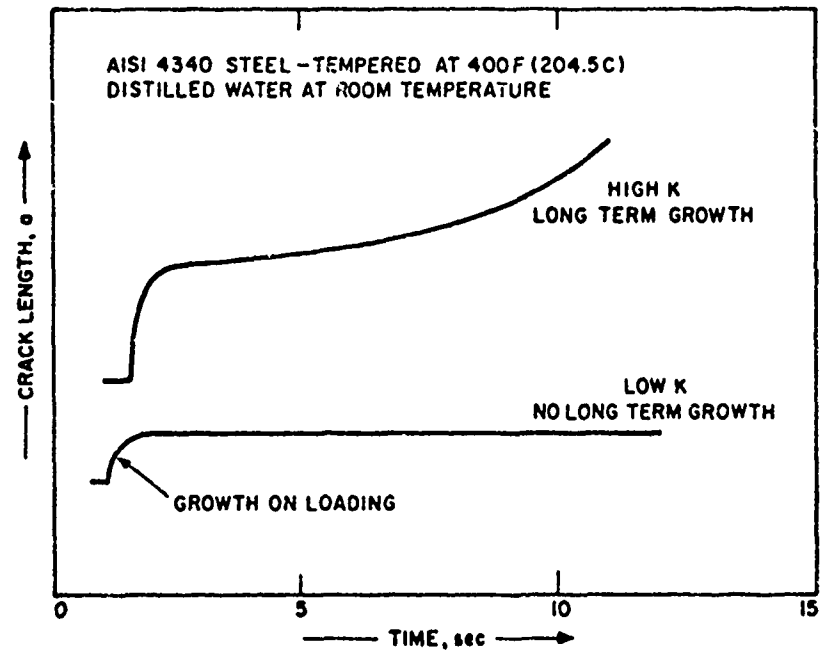

A. Schematic illustration of crack extension on loading and initial transient crack growth. (21)

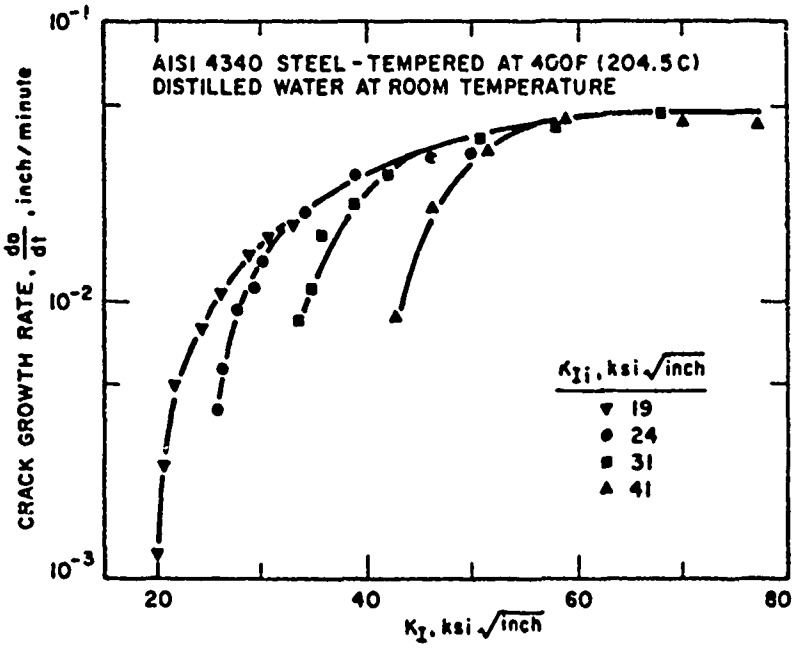

B. Kinetics of sustained load crack growth showing the nonsteady state effect of initial K_I (21)

Figure 10. Illustration of nonsteady state crack growth rate phenomena.

Typical steady-state crack growth responses as a function of K_I are illustrated by the results of Wei et al (21), Figure 11A, and is also shown schematically in Figure 11B. Steady-state crack growth kinetics may be divided into three regions. Region I is highly dependent on K_I, and may reflect crack acceleration for certain types of tests. Region II is nearly independent of K_I and represents a range where crack growth is limited by the embrittling chemical process. In Region III, crack growth approaches the condition for unstable growth. For high strength materials, under conditions approximating plane-strain, the condition for the onset of unstable growth is defined by $K_I = K_{Ic}$.

The interpretation and analysis of the sustained load crack growth kinetics developed during the present investigation must include careful consideration of nonsteady-state crack growth if effective quantitative estimates are to be made to explain corrosion fatigue. The existence of an incubation period and nonsteady crack growth can lead to an underestimation of the steady-state rate of crack growth, with a consequential over estimation of the safe operating lives of components utilized in corrosive media.

The sustained load crack growth kinetics obtained for 4340 steel tested in distilled water at 32°F, 70°F, and 212°F are shown in Figure 12 plotted as a function of instantaneous K_I, calculated as the crack length increases. Each data point represents the steady-state crack growth condition for at least 10 tests conducted at various applied K_I and determined from plots similar to those presented in Figure 10B. These kinetics are characteristic of Region II, Figure 11b, nearly independent of K_I but strongly dependent upon the environmental temperature. As indicated by these data the surface reaction promoting entrance of hydrogen into the specimen is considerably enhanced as temperature is increased.

Presenting these data on log-log plots, Figure 13, and representing them in terms of the commonly used relationship:

$$\frac{da}{dt} = A\, K_I^{\,n}$$

revealed that the exponent n is strongly dependent upon the environmental temperature and that the relationship does not adequately predict crack growth kinetics over the entire range of K_I.

As crack growth approaches the condition for unstable growth, high values of instantaneous K_I, the relationship is particularly unsatisfactory. For steady-state crack growth, however, da/dt is a fairly direct function of instantaneous K_I and temperature, and provided that the exponent n has been established for a particular environment and temperature, the relationship can be useful for making engineering estimates of crack growth kinetics.

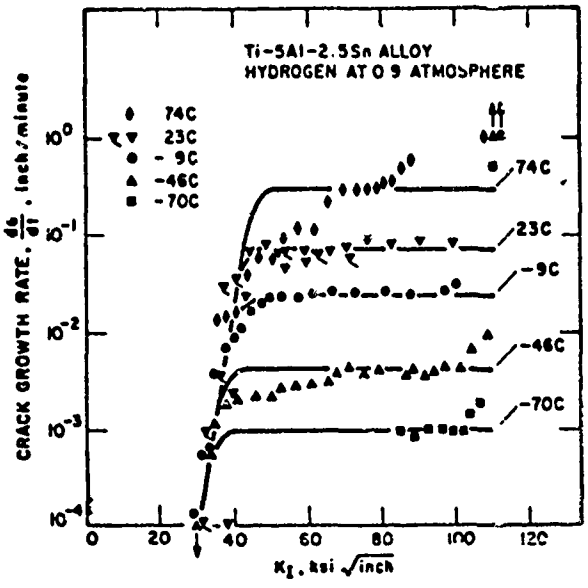

A. Typical steady-state crack growth kinetics (21)

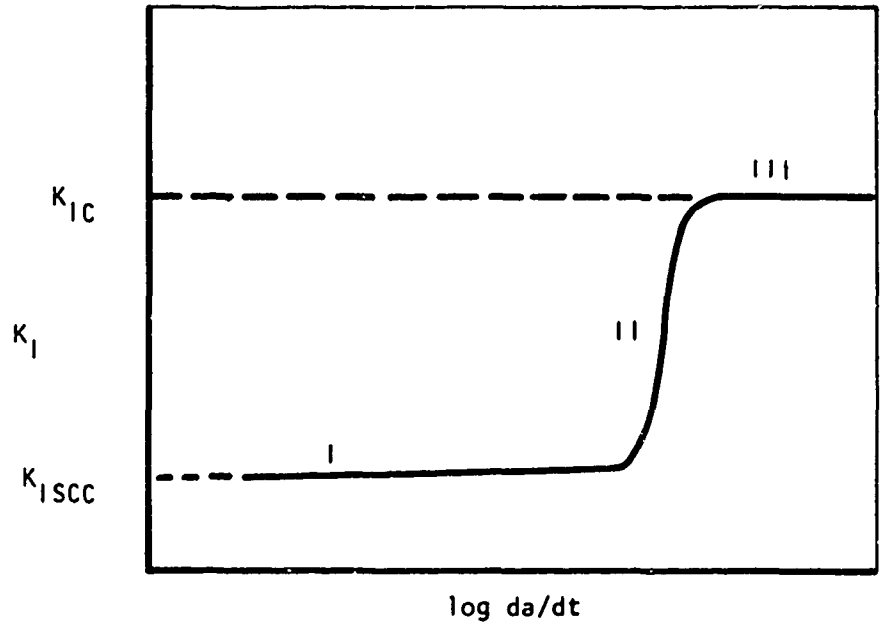

B. Schematic representation of steady state crack growth kinetics (21)

Figure 11. Illustrations of steady state crack growth kinetics.

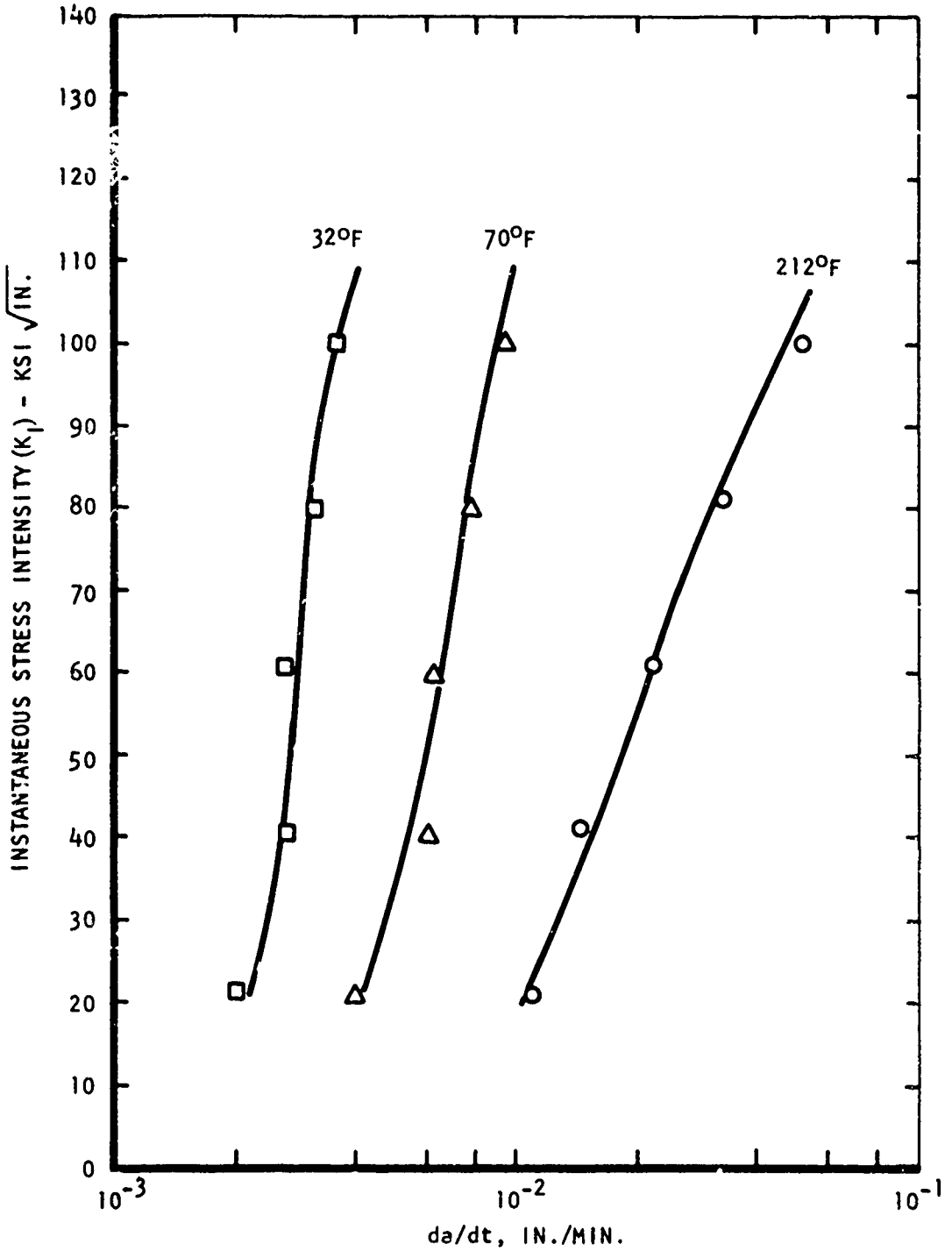

Figure 12. Crack growth kinetics for precracked 4340 steel tested in distilled water at 32°F, 70°F, and 212°F.

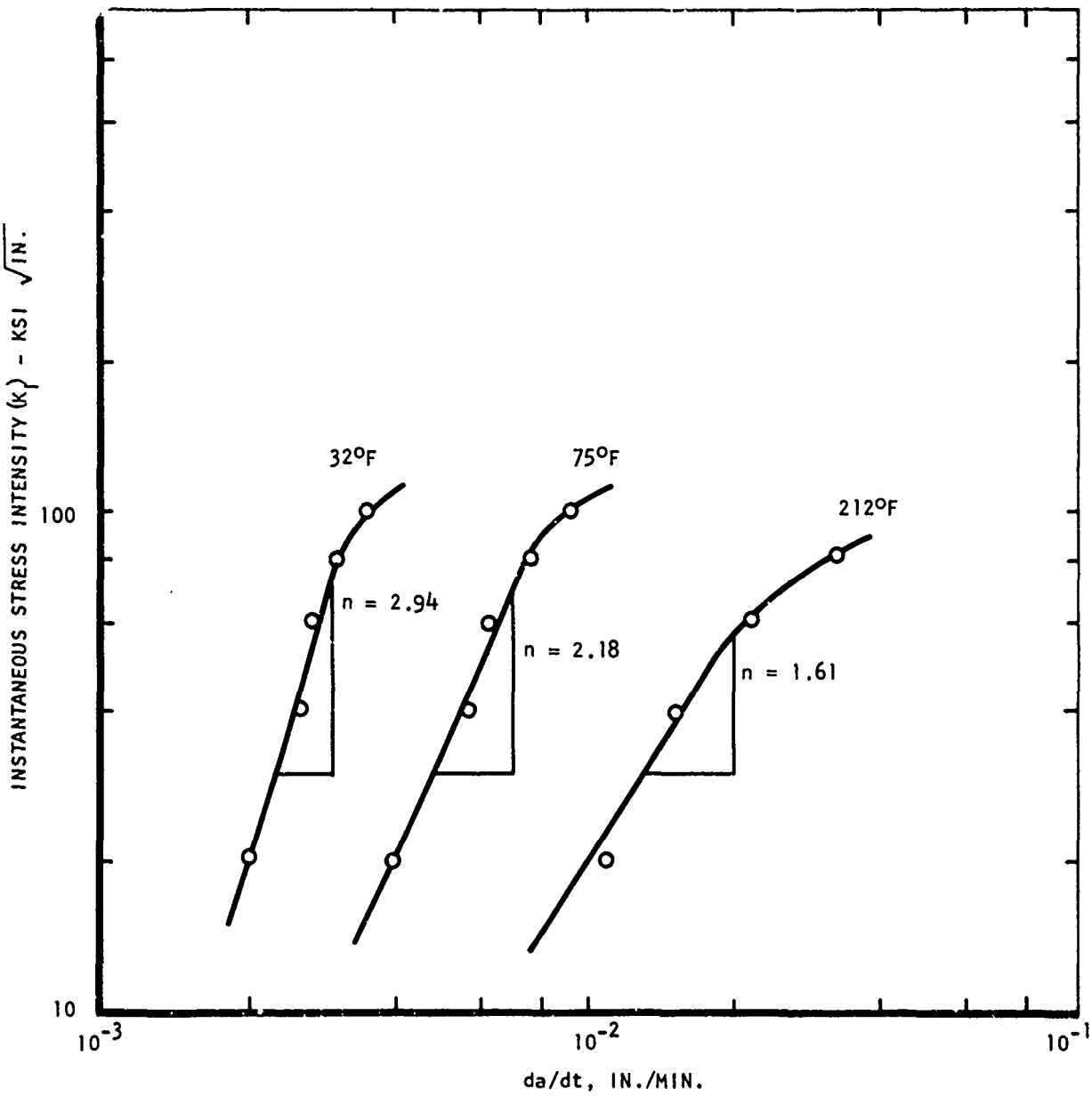

Figure 13. Crack growth kinetics for precracked 4340 steel tested in distilled water at 32°F, 70°F, and 212°F, compared to a da/dt = AK^n type relationship.

4. Stress Corrosion Cracking Activation Energy

The activation energies for both stress corrosion crack growth rate and failure time under sustained loads were determined by plotting the logarithm of the growth rate and failure time as a function of the reciprocal of the absolute temperature. The results for crack growth rates at various instantaneous K_I, obtained from Figure 12, are shown in Figure 14. For comparative purposes the 5200 cal/mole which would correspond to the activation energy for hydrogen adsorption onto a clean iron surface (26) and 9000 cal/mole which correspond to the activation energy for diffusion of hydrogen through a lattice (5,27-29) are also presented in the figure. Some variation in activation energy occurs as a function of instantaneous K_I, ranging from 4450 cal/mole at 70 ksi $\sqrt{in.}$ to 3930 cal/mole at 20 ksi $\sqrt{in.}$, but comparison with the 5200 cal/mole value for surface adsorption of hydrogen yields closer agreement than for hydrogen diffusion through a lattice.

On this basis the results lend additional support to the conclusion of Steigerwald and Kortovich (12) that stress corrosion crack growth of 4340 in distilled water is controlled by a surface reaction permitting hydrogen to enter the specimen (12). These results do not, however, agree with those of Johnson (31) and Van der Sluys (32), who observed activation energies of approximately 9000 cal/mole, corresponding to the diffusion of hydrogen through a lattice. Additional work is required to clarify the exact mechanism operative here.

B. Environmentally-Accelerated Fatigue Crack Growth

The principal feature of corrosion fatigue attack is the ease with which the combined fatigue-environmental action will nucleate and propagate cracks. To determine the general character of corrosion-fatigue crack growth behavior, the frequency of cyclic loading and temperature were varied for 4340 steel tested in distilled water. If the environmental damage is time dependent and if the fatigue damage is cycle dependent, then variation of frequency allows the time-dependent action to occur while it holds the cycle-dependent action constant, and suggests that frequency of applied load could play the leading role in describing the interaction between the fatigue and environmental processes.

1. Frequency Effects

The frequency effects were determined by fatigue tests conducted under load controlled conditions in distilled water at 32°F, 70°F, and 212°F. Two load ranges were used, 2000-4000 pounds, and 2000-5000 pounds. For the geometry of the precracked compact K_{Ic} specimens used for these tests, K_{Imin} was approximately 20 ksi $\sqrt{in.}$ which was just above the K_{Iscc} for this material at each test temperature. These tension-tension load range conditions were selected with K_{Imin} close to K_{Iscc} to determine if long incubation times would have an effect upon the predictability of the superposition principle. The fatigue crack growth kinetics as a function of instantaneous K_{Imax} are shown in Figures 15, 16, and 17.

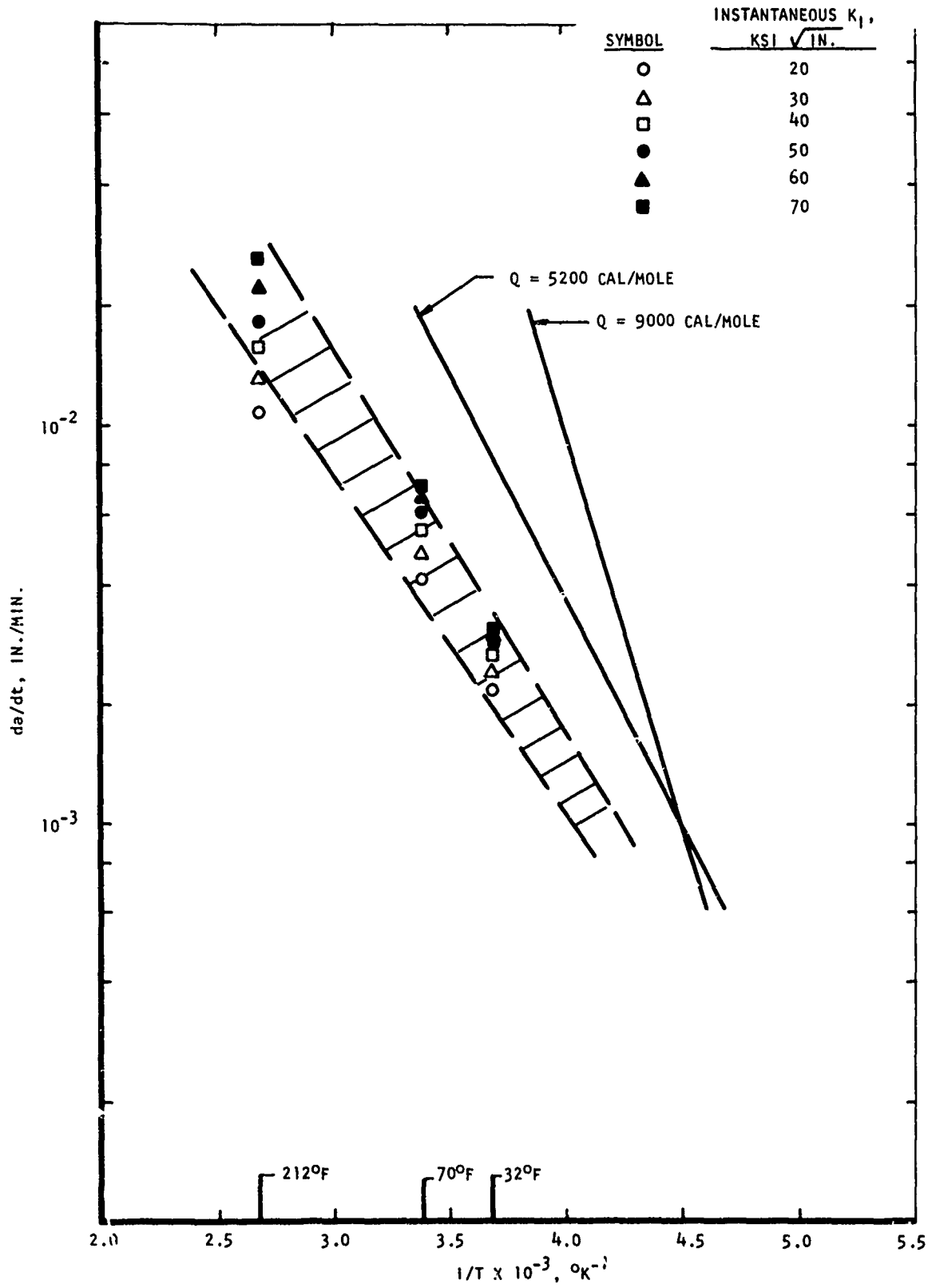

Figure 14. Activation energy for crack growth kinetics of 4340 steel tested in distilled water.

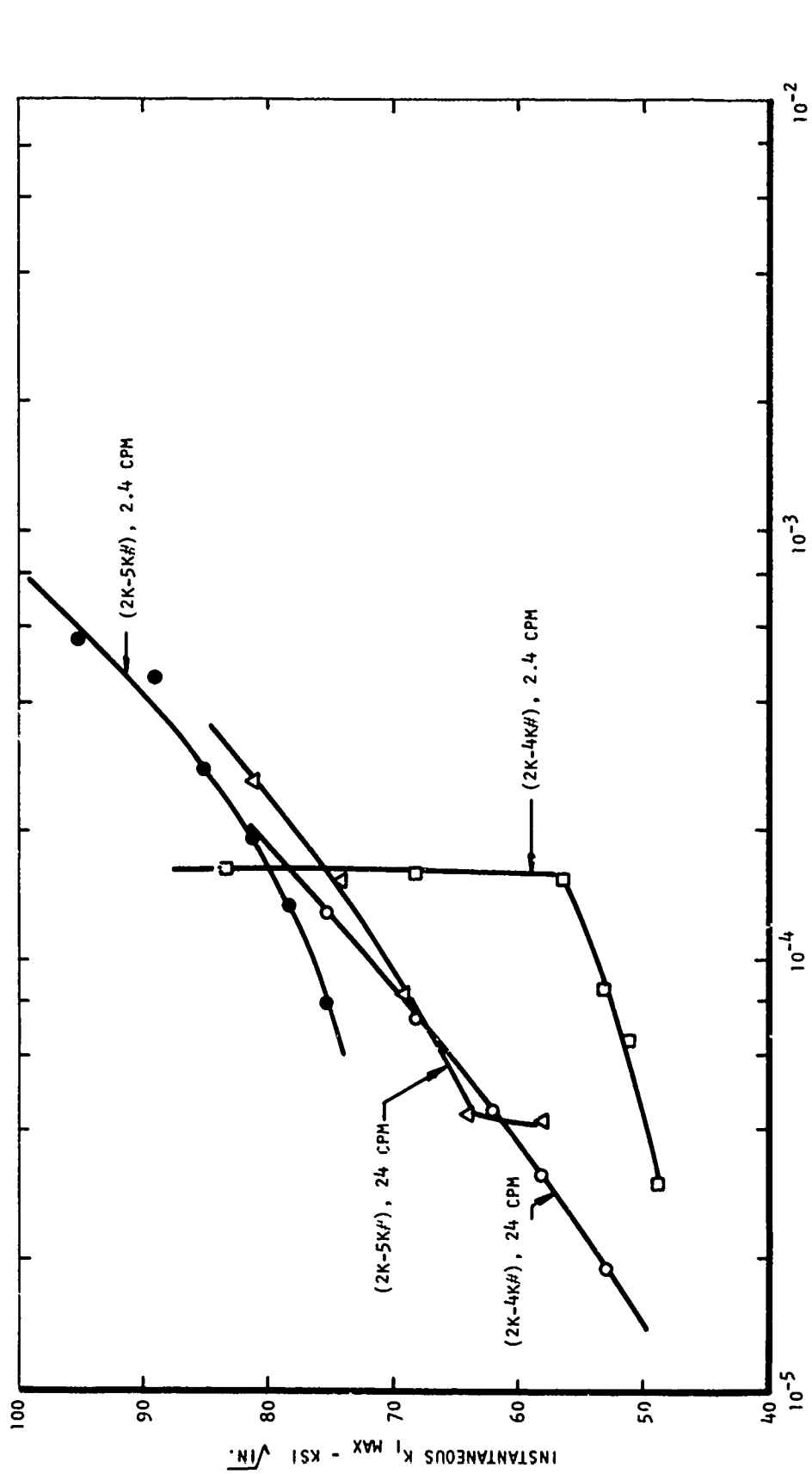

Figure 15. Fatigue crack growth rate for 4340 steel tested in distilled water at 32°F, two load ranges, and two frequencies.

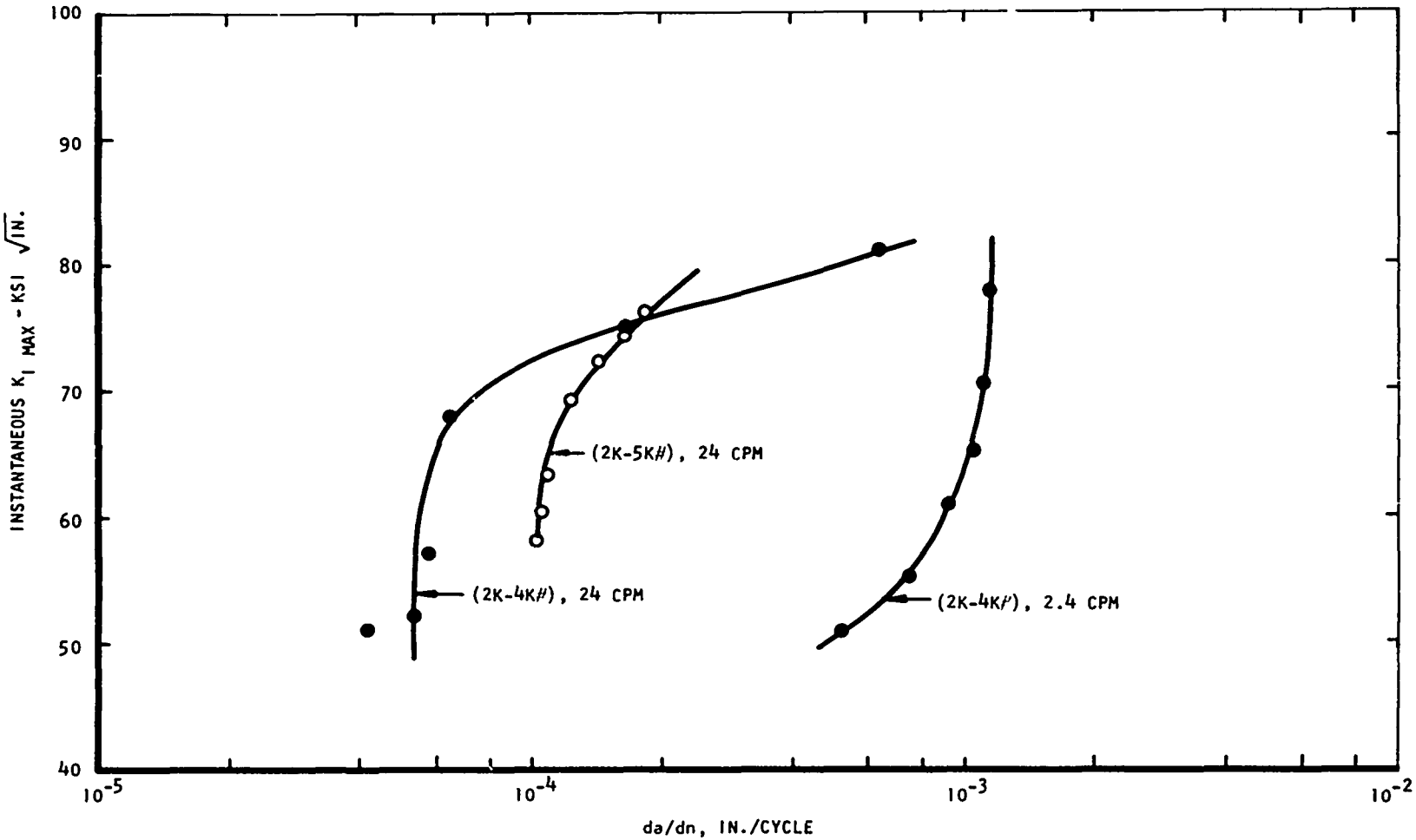

Figure 16. Fatigue crack growth rate for 4340 steel tested in distilled water at 70°F, two load ranges, and two frequencies.

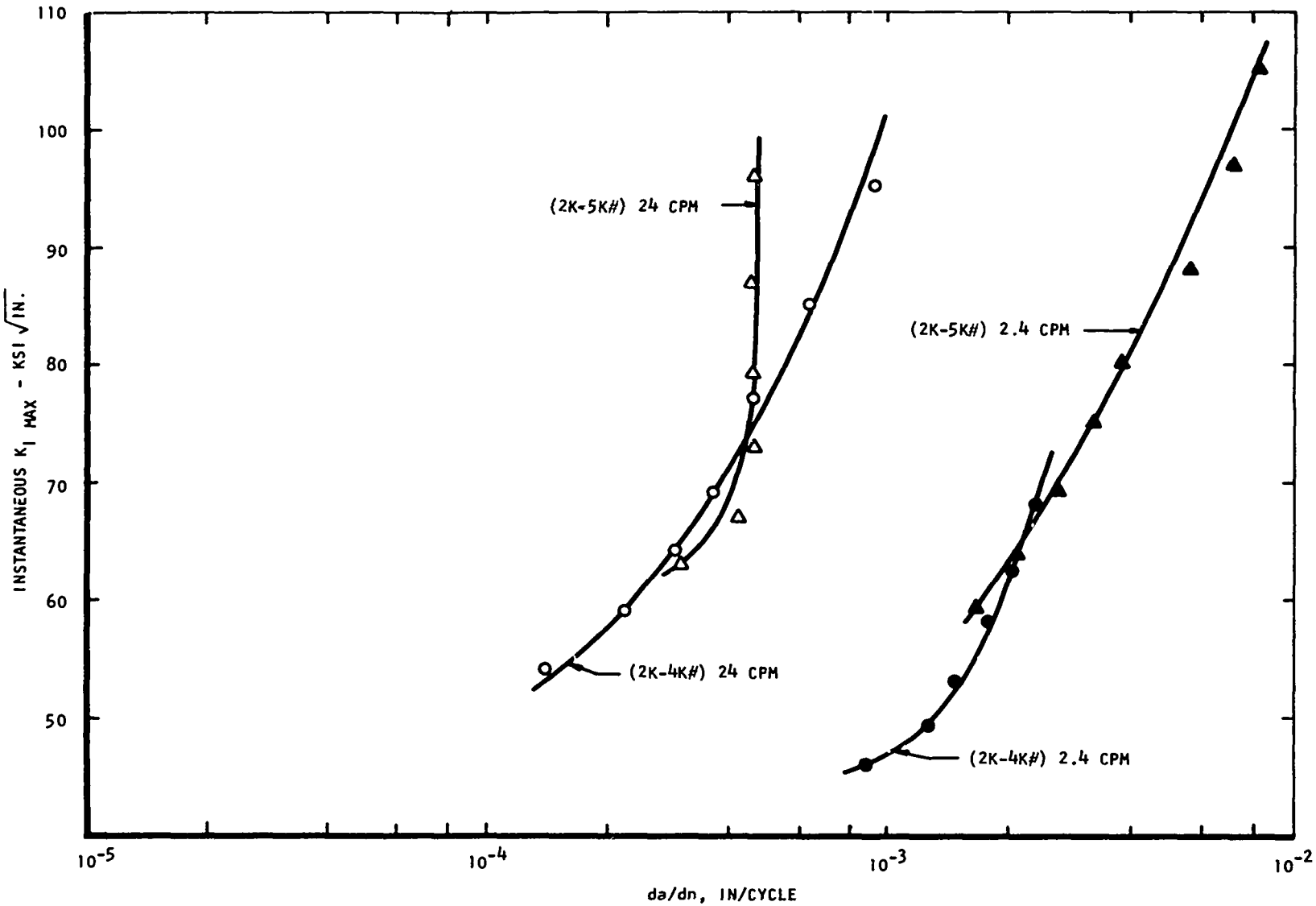

Figu e 17. Fatigue crack growth rate for 4340 steel tested in distilled water at 212°F, two load ranges, and two frequencies.

As shown in Figures 16 and 17, the 70°F and 212°F test temperatures, frequency of applied load and environment temperature had a considerable effect upon the interaction between the fatigue and environmental processes. As frequency decreased the crack growth rate increased in magnitude for both temperatures indicating that the time-dependent action of the corrosive environment has more influence than the cycle dependent fatigue damage alone. At 212°F the load range did not have an appreciable effect upon the resultant crack growth rate, while at 70°F, Figure 16, the higher load range (for 24 cpm) produced slightly higher crack growth rates.

The results for tests conducted at 32°F, Figure 15, were not as conclusive. Aside from tests at the lower load range conducted at 2.4 cpm, crack growth rate was independent of test frequency and load range, indicating very little dependency upon the time-dependent action of the corrosive environment.

2. Predictability of Experimental Results

Wei and Landes (19) have recently proposed a linear summation hypothesis which suggests that environmentally induced fatigue crack propagation rates can be directly obtained by adding the cyclic crack growth rates due to the individual mechanisms of environmental attack and environmentally independent fatigue. This hypothesis was suggested to apply only above K_{Iscc} because, by definition, there is no sustained load crack growth below K_{Iscc} (30). In order to apply this predictability criterion to the corrosion fatigue of 4340 in distilled water, cycle dependent fatigue data were obtained in an atmosphere of dehumidified argon at room temperature. The assumption is made here that the crack growth rate in the argon reference atmosphere is independent of temperature. The fatigue crack growth kinetics as a function of instantaneous stress intensity K_{Imax} are shown in Figures 18-20. Included in these figures are the predicted curves utilizing the Wei-Landes analysis (19).

A basic difference exists between the shapes of curves developed in the argon reference atmosphere and those obtained in the distilled water environment. The argon curves are more indicative of Region III type behavior, (22), in which the crack growth rate is quite sensitive to the maximum value of stress intensity and increases sharply for small changes in K_{Imax}. The corrosion fatigue curves, on the other hand, are more characteristic of Region II behavior, where crack growth rate increases more slowly with increases in K_{Imax}. In addition, there is a relatively small effect of frequency when no environment is present, indicating that fatigue damage is more cycle dependent than time dependent.

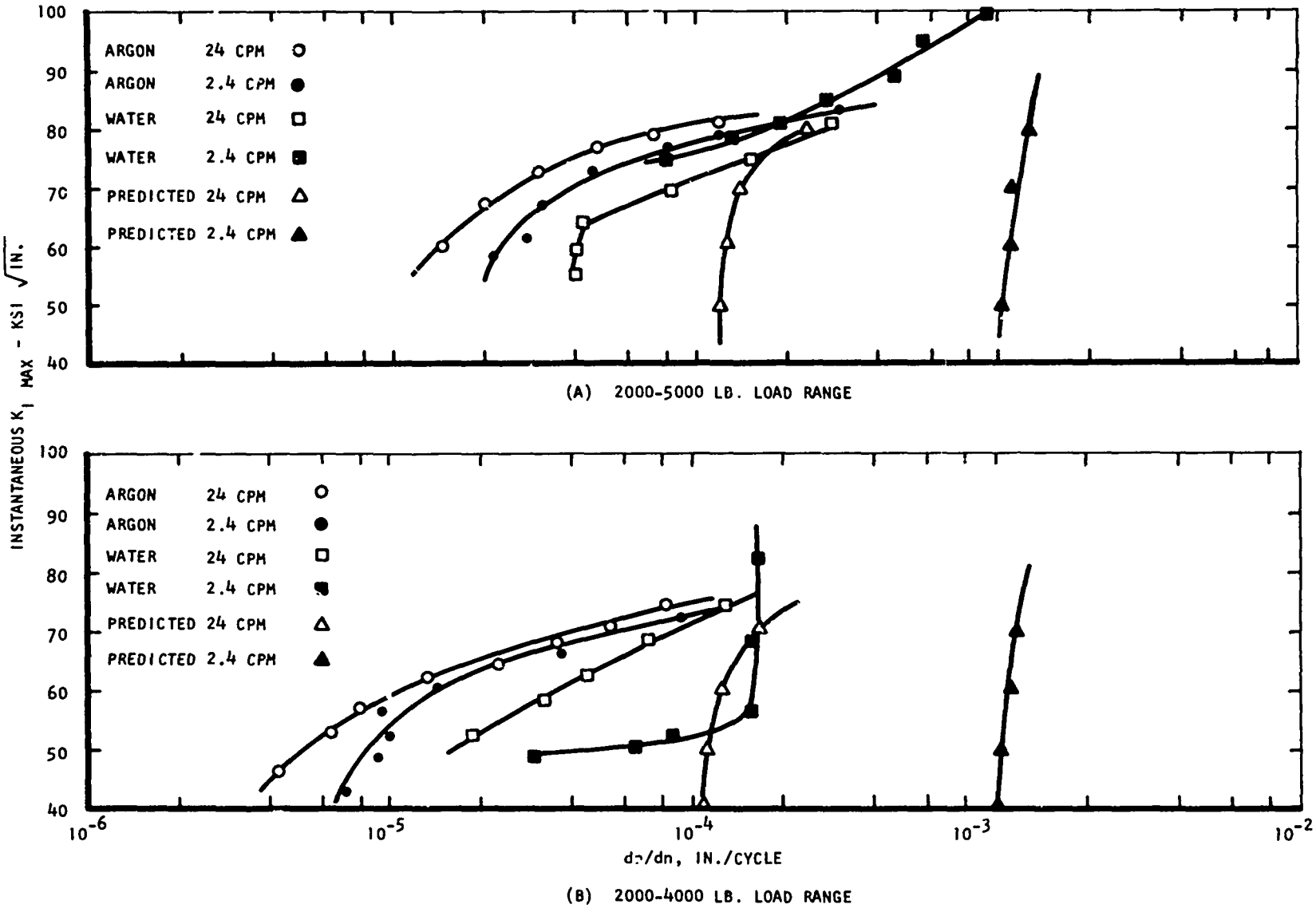

Figure 18. Fatigue crack growth rate for 4340 steel tested in distilled water at 32°F and argon at 70°F, two load ranges, and two frequencies compared to Wei-Landes predictions.

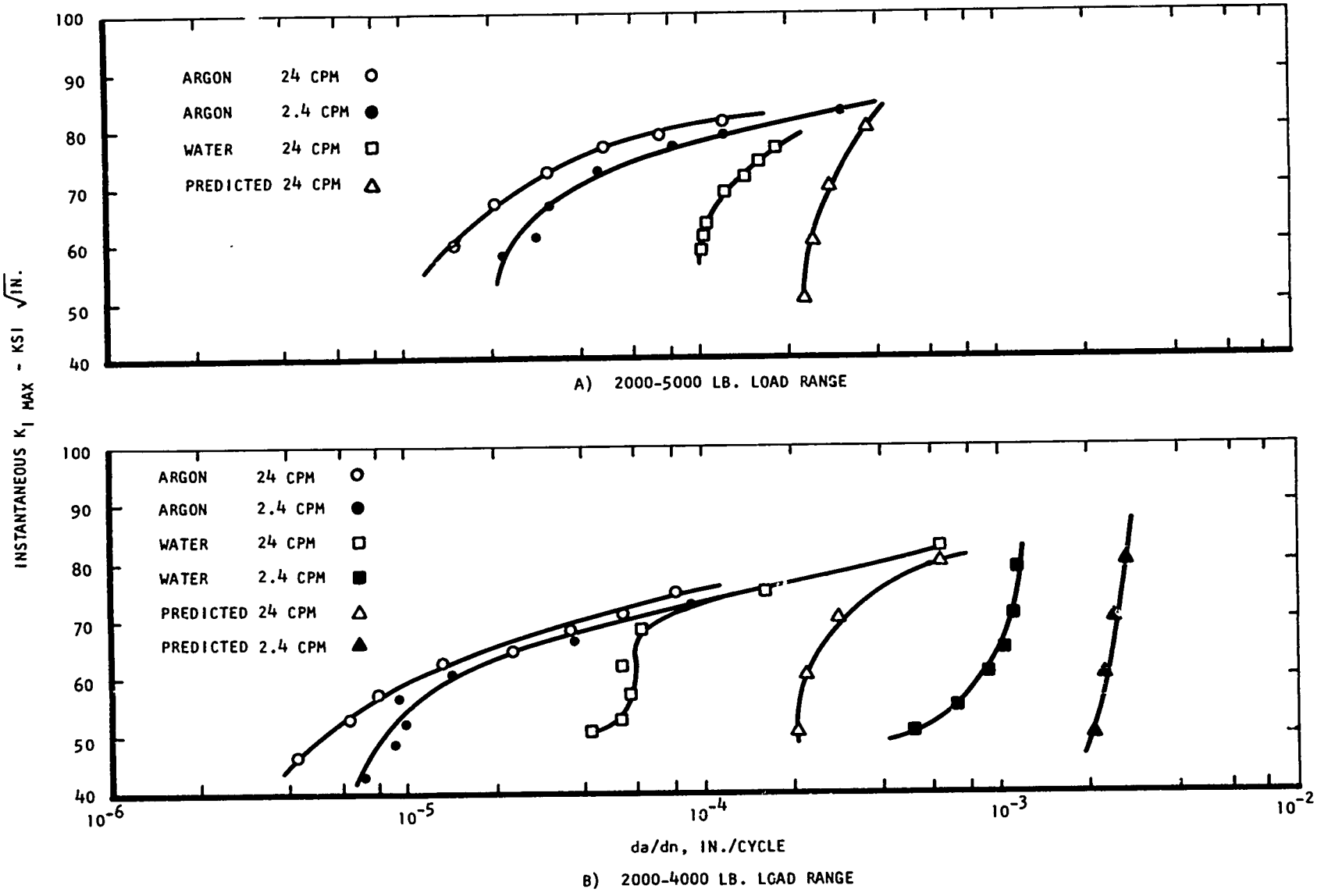

Figure 19. Fatigue crack growth rate for 4340 steel tested in distilled water and argon at 70°F, two load ranges, and two frequencies compared to Wei-Landes predictions.

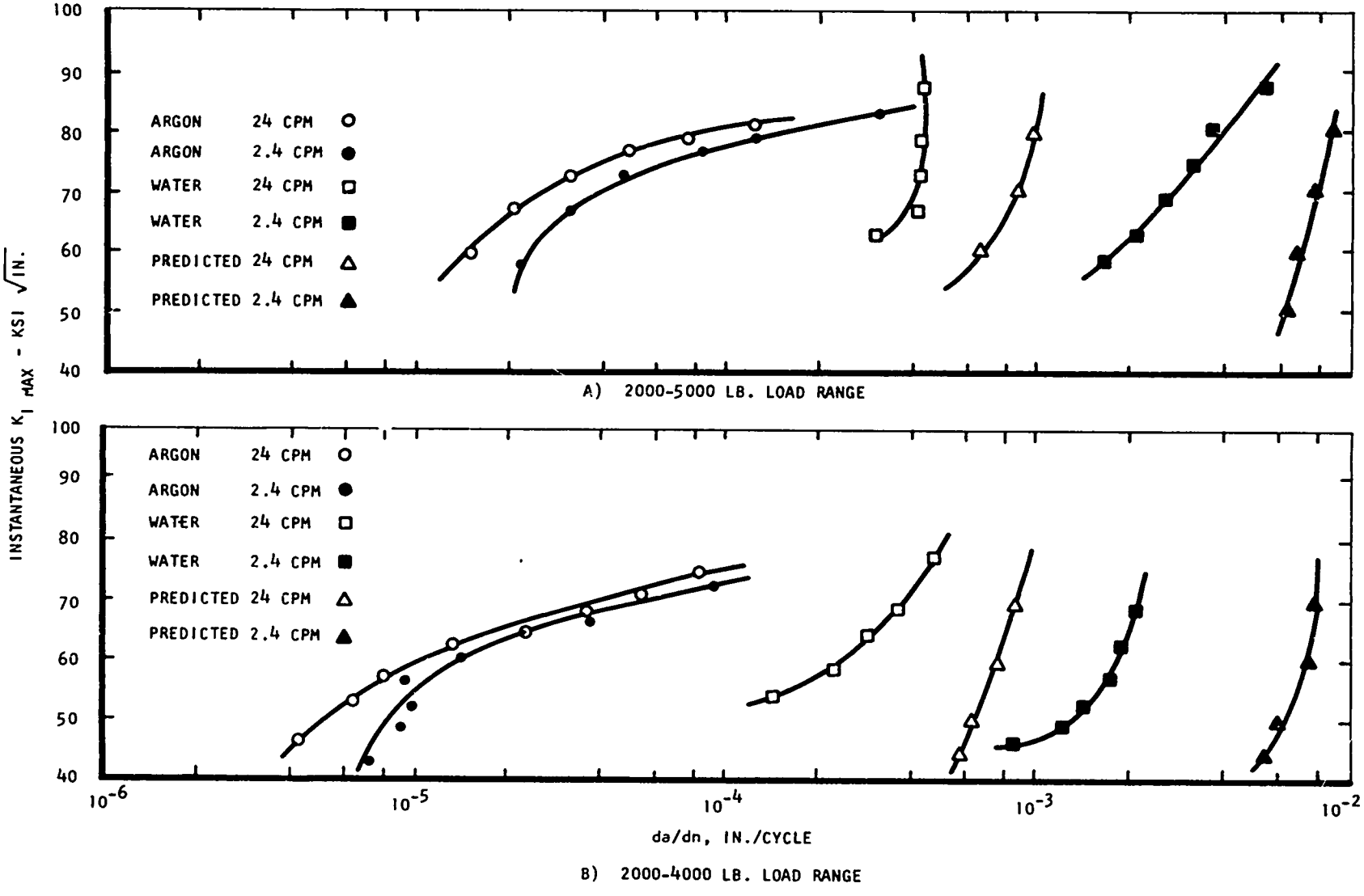

Figure 20. Fatigue crack growth rate for 4340 steel tested in distilled water at 212°F and argon at 70°F, two load ranges, and two frequencies compared to Wei-Landes predictions.

Comparison of the argon curves with the corrosion fatigue curves illustrates the degrading influence of the environment, becoming more pronounced as frequency decreases and temperature increases. With the exception of the tests conducted at 32°F, Figure 18, the corrosion fatigue crack growth rates are at least one order of magnitude greater than the cycle-dependent argon fatigue crack rates at any given frequency. These data suggest that the fatigue process has a negligible effect on the crack advance during the load cycle in corrosion fatigue and that the rate of crack growth will be controlled primarily by environmental attack. With the exception of tests conducted at the low load range and 2.4 cpm frequency, however, the effect of environment at 32°F was quite small presumably because the stress corrosion kinetics were slow.

Application of the Wei-Landes analysis to the corrosion fatigue crack growth data resulted in poor predictability. In all instances the predicted crack growth rates were significantly higher than the experimental results. Since it has been concluded that crack growth is controlled predominantly by the environmental attack, the contribution of the environmental component computed from sustained-load crack growth data is too high. The Wei-Landes analysis (19), Figure 21 , predicts the fatigue crack growth rate in an environment to be a summation of a mechanical component $da/dn]_R$ determined from fatigue tests in a reference environment plus an environmental component $\int da/dt[k(t)]dt$ computed from the crack growth rate determined under sustained load. Procedurally, a crack velocity versus time curve, Figure 21C, is constructed on the basis of the stress-intensity spectrum, Figure 21A, and the sustained-load crack-growth data, Figure 21B. The area under this curve may then be determined graphically or numerically to give the environmental contribution for the particular K spectrum. The environmental component at each K level is then added algebraically to the corresponding rate of fatigue crack growth in the reference environment to produce the requisite environment enhanced fatigue crack growth curve, Figure 21D.

A basic assumption of this model is the precept that crack growth does not commence until K_{Iscc} has been exceeded at some point in the load profile. However, studies have shown that incubation time effects may be significant at K_{Imin} close to K_{Iscc}, resulting in a more complex relationship between da/dt and K_I than determined from sustained load tests. In addition, agreement between the predicted curves and experimental results for a stress ratio $R = K_{min}/K_{max} = .8$ was not good (21), suggesting that at the higher stress ratio, higher K prevails over each fatigue cycle and produces a greater contribution from the environmental component. All of this indicates that the contribution from the environment may, in fact, be more complicated than that predicted on the basis of the stress intensity spectrum and the sustained load crack-growth data.

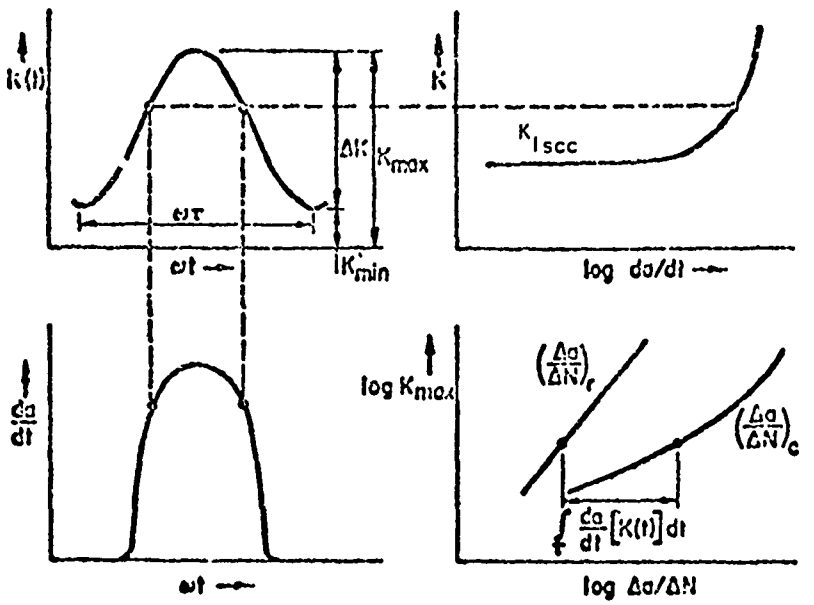

Figure 21. Schematic diagram illustrating the Wei-Landes method of analysis. (A) stress intensity spectrum in fatigue (top left); (B) rate of crack growth under sustained load in an aggressive environment (top right); (C) environmental contribution of crack growth in fatigue (bottom left); and (D) integrated effects on environment and K_{max} on fatigue crack growth rate (bottom right) (19).

In the present investigation, although K_{Imin} was above K_{Iscc}, and should theoretically, have offered some contribution to crack growth, a prediction was made omitting the contribution of applied K_I until K_{Imin} had been exceeded. In each instance, predictability was improved by the utilization of this assumption, Figures 22-24. A schematic illustration of this assumption and the Wei-Landes counterpart are shown in Figure 25. According to the Wei-Landes model, the entire area under the da/dt versus time curve represents the environmental component to fatigue crack growth per one cycle of loading. Utilization of the entire area under the curve resulted in higher crack growth rates than observed experimentally. By eliminating the contribution below K_{Imin}, predictability was enhanced.

There is some physical justification for this assumption, Figure 23B, but it is stressed that this is purely qualitative in nature, and is offered only as a first approximation. As cyclic loading proceeds, each load profile produces elastic strain in the material, except at the crack tip itself where a small volume of material may undergo plastic strain. During the unload portion of the fatigue cycle, as the elastic strain is released and the mateiral tends towards its original state of stress, a compressive stress may be imparted to this plastic zone. On a macroscale, this has the effect of lowering the apparent K_I imparted to the specimen. This reduction would decrease the environmental contribution towards da/dn. The exact function of the contribution is complex and it is emphasized that the assumption to omit the portion of da/dt below K_{Imin} is only a first approximation. Although further development and experimental verification of this method is needed it is apparent that when tension-tension loading rather than tension-compression loading is used the Wei-Landes model can significantly overestimate the crack growth rate presumably due to residual stress effects at the crack tip. These residual stresses can then mitigate the contribution of the mean load to the stress corrosion process.

3. Corrosion Fatigue Cracking Activation Energy

The activation energy for corrosion fatigue crack growth rate was determined by plotting the logarithm of the growth rate as a function of the reciprocal of the absolute temperature. The results for crack growth rates at two different frequencies, obtained from Figures 18-20 are shown in Figure 26. For comparative purposes the 5200 cal/mole which corresponds to the activation energy for hydrogen adsorption onto a clean iron surface (26) and the 9000 cal/mole which corresponds to the activation energy for diffusion of hydrogen through a lattice (5,27-29) are also presented in the figure. Results for tests conducted at 24 cpm (Q = 4560 cal/mole) are linear, while more variability was observed for tests conducted at 2.4 cpm (Q = 4560 cal/mole). These values are more closely associated with the 5200 cal/mole value for surface adsorption of hydrogen than for hydrogen diffusion. Since the corrosion fatigue crack growth rates were observed to depend primarily upon the environmental contribution to growth rate, Figures 18-20, and the activation energies obtained from sustained-load tests indicated that kinetics in precracked specimens were

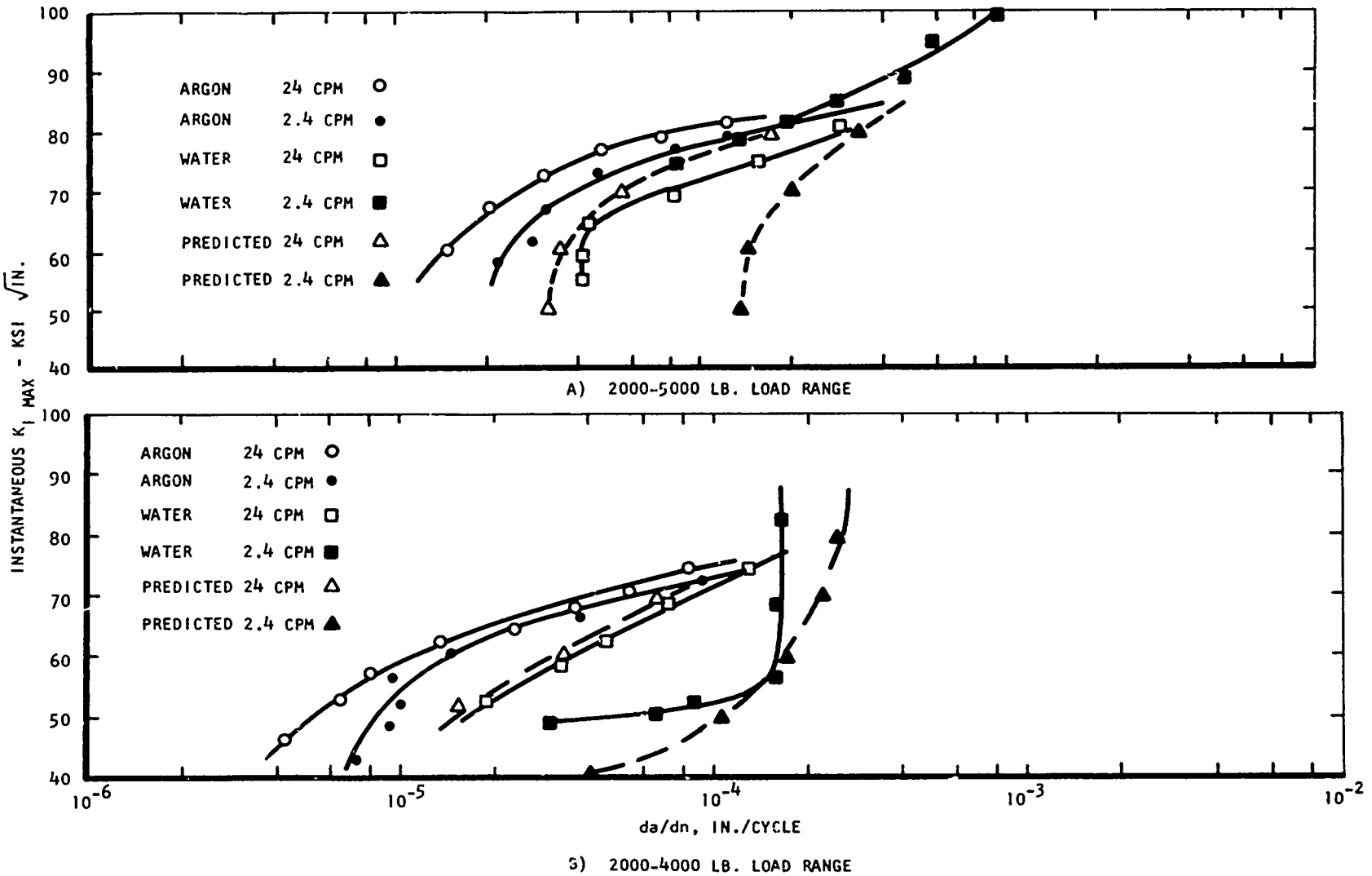

Figure 22. Fatigue crack growth rate for 4340 steel tested in distilled water at 32°F and argon at 70°F, two load ranges, and two frequencies compared to modified Wei-Landes predictions.

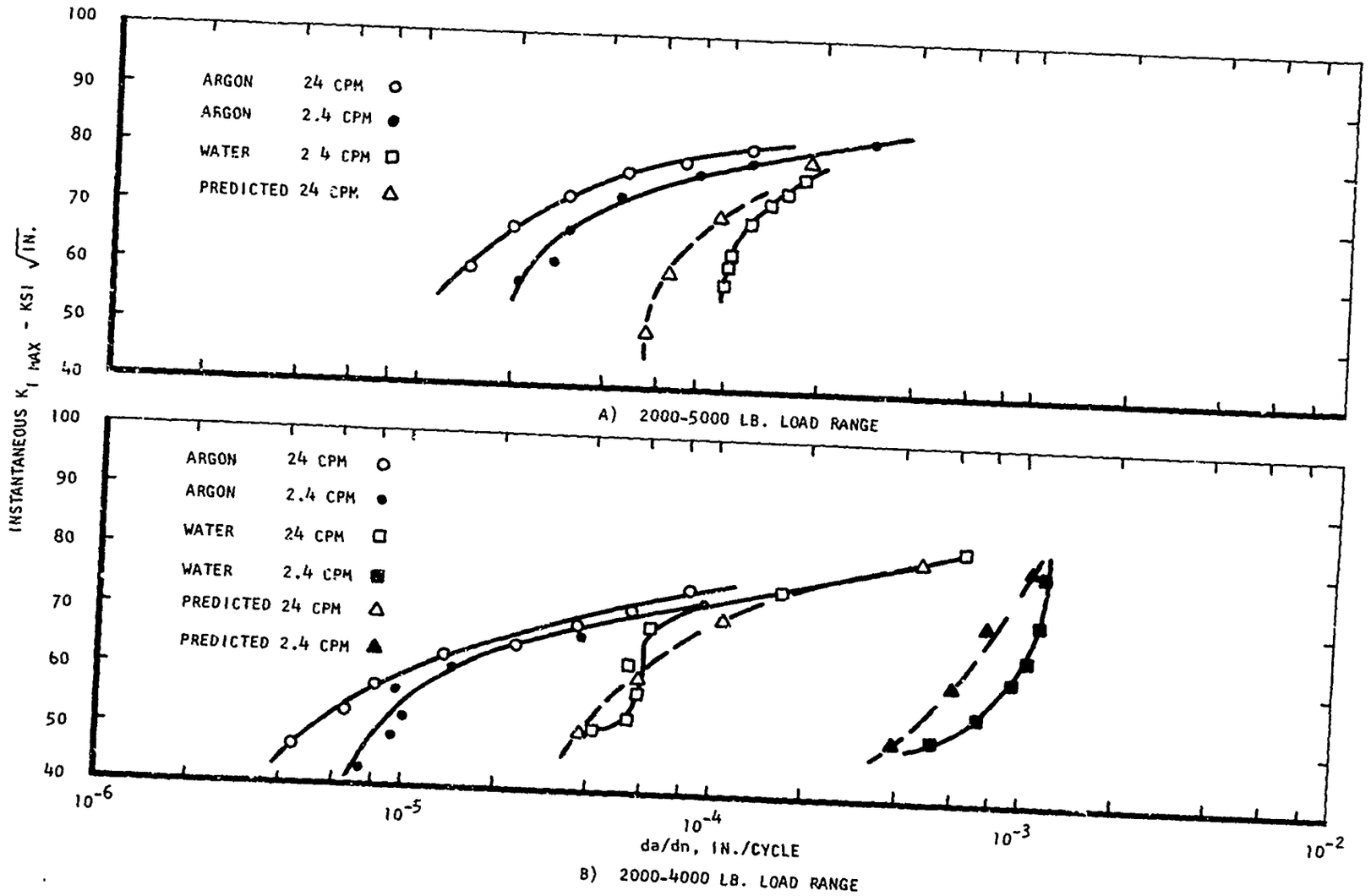

Figure 23. Fatigue crack growth rate for 4340 steel tested in distilled water and argon at room temperature, two load ranges, and two frequencies compared to modified Wei-Landes predictions.

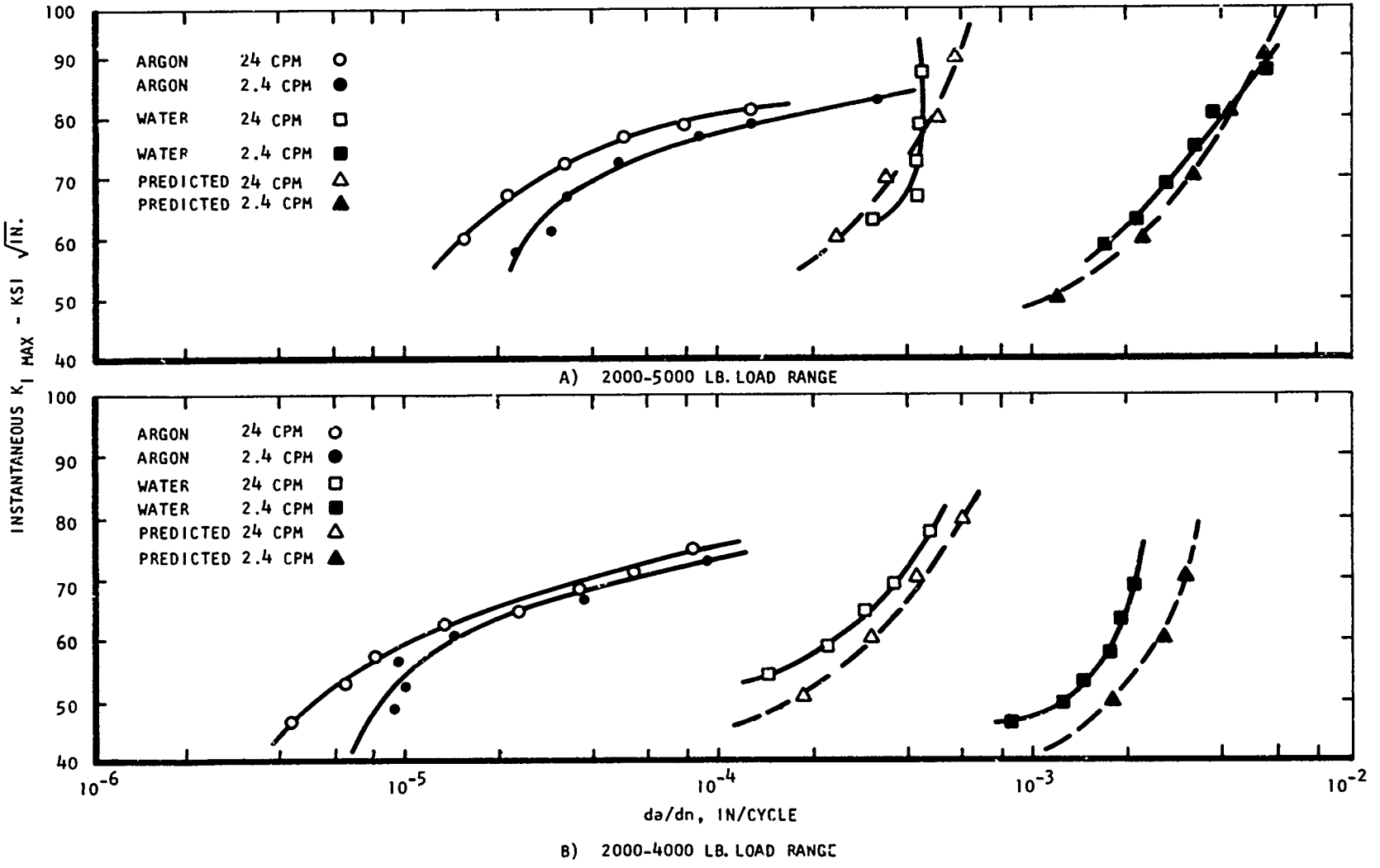

Figure 24. Fatigue crack growth rate for 4340 steel tested in distilled water at 212°F and argon at 70°F, two load ranges, and two frequencies compared to modified Wei-Landes predictions.

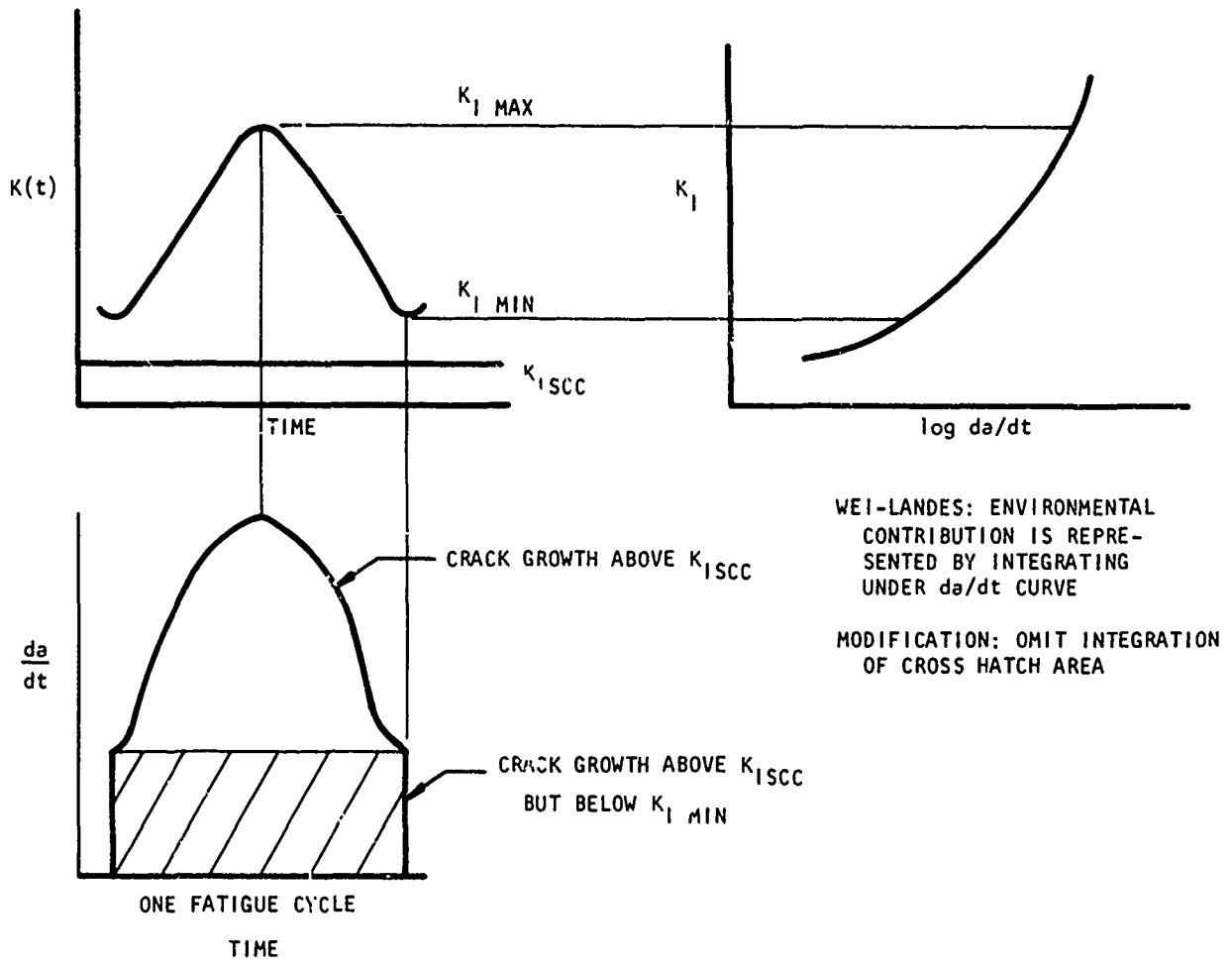

A) SCHEMATIC ILLUSTRATION OF WEI-LANDES ANALYSIS (19) MODIFICATION

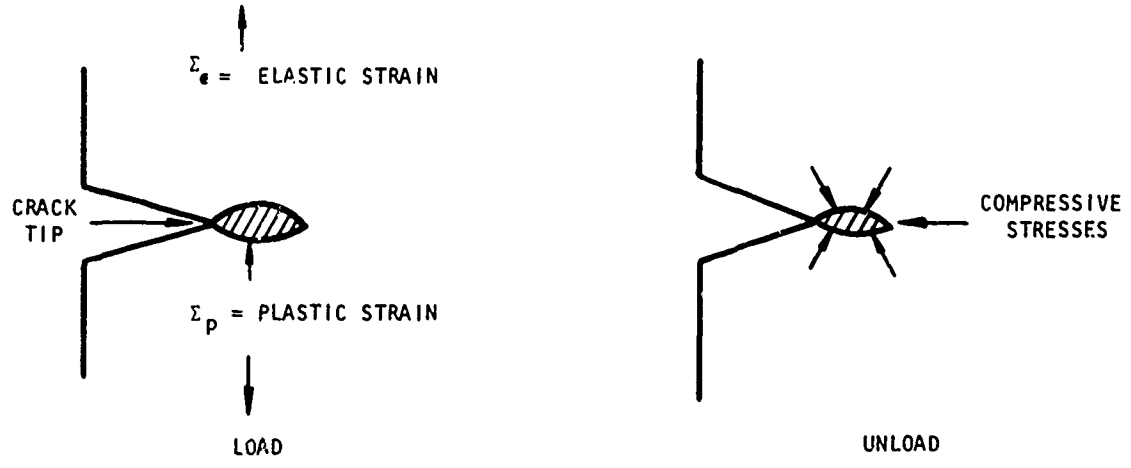

B) PHYSICAL JUSTIFICATION (SEE TEXT FOR DISCUSSION)

Figure 25. Schematic illustration of and physical justification for modification to Wei-Landes analysis.

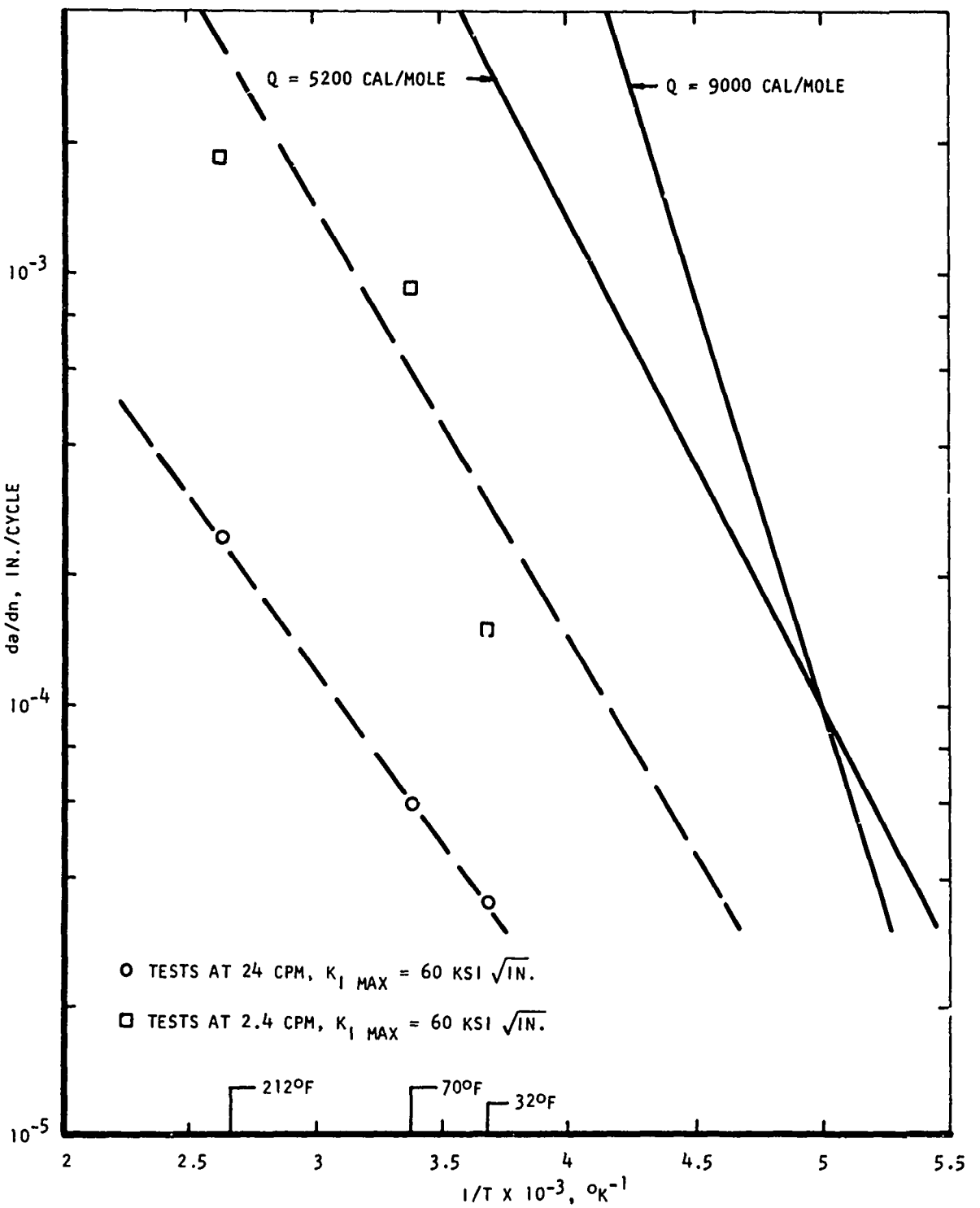

Figure 26. Activation energy for corrosion fatigue crack growth kinetics of 4340 steel tested in distilled water, load range = 2000-4000 pounds.

associated with surface adsorption, it is concluded that the corrosion fatigue crack growth of 4340 in distilled water is dependent upon the particular surface reaction permitting hydrogen to enter the specimen.

IV - SUMMARY AND CONCLUSIONS

Experiments were conducted to study the corrosion fatigue of high strength AISI 4340 steel above K_{Iscc} in a distilled water environment and to determine whether or not the Wei-Landes superposition model could accurately predict crack growth behavior. This model considers the acceleration of fatigue cracking in an aqueous environment as a superposition of the crack growth characteristics under sustained load on the crack growth kinetics obtained in fatigue in inert environments. In order to evaluate this model, sustained load tests were conducted in a distilled water environment and were combined with fatigue tests conducted in an argon atmosphere to predict the corrosion fatigue crack growth rate in distilled water.

Delayed failure curves for sustained load tests conducted at 32°F, 70°F, and 212°F in a distilled water environment where characteristic of those of hydrogenated high strength steels in that (1) cracking proceeded discontinuously until a critical length was attained followed by rapid failure, (2) failure time varied only slightly with applied stress intensity, and (3) a lower critical stress (K_{Iscc}) was obtained below which delayed failure was not observed.

The severity of environmental embrittlement was quite temperature sensitive. Both failure time and K_{Iscc} decreased as temperature increased, indicating that the corrosion reaction occurring at the surface became more aggressive. The sustained load steady-state crack growth kinetics were nearly independent of K_I but strongly dependent on the hydrogen generating process at the crack surface, particularly as affected by the environmental temperature. For steady-state crack growth the commonly used relationship:

$$\frac{da}{dt} = A\, K_I^{\,n}$$

accurately predicted da/dt until the onset of unstable crack growth. The exponent n was observed to be temperature sensitive and decreased as temperature increased.

The activation energy for the stress corrosion crack growth rate under sustained loads compared more favorably with the 5200 cal/mole activation energy for hydrogen adsorption onto a clean iron surface than for hydrogen diffusion. On this basis the results lend additional support to the conclusion that stress corrosion crack growth of the 4340 in distilled water is controlled by the surface reaction permitting hydrogen to enter the specimen.

The environmentally accelerated fatigue crack growth rate was frequency and temperature sensitive. As frequency decreased and temperature increased, the crack growth rate increased in magnitude indicating that the time-dependent action of the corrosive environment had more influence than the cycle dependent fatigue damage alone. The results for tests conducted at 32°F were not as definitive, indicating in general that there was very little dependency upon the time dependent action of the corrosive environment at this temperature.

Comparison of the crack growth kinetics for environmentally accelerated fatigue with those for fatigue in the inert dehumidified argon atmosphere illustrated the degrading influence of the environment. The effect, with the exception of certain 32°F distilled water tests, became more pronounced as frequency decreased and temperature increased. At any given frequency the corrosion fatigue crack growth rates were at least one order of magnitude greater than the cycle dependent argon fatigue growth rates, indicating that the kinetics are controlled primarily by environmental attack.

Application of the Wei-Landes model to the corrosion fatigue crack growth data predicted growth rates that were higher than observed. By modifying this analysis to exlude any environmental contribution to crack growth rate below the applied $K_{I\min}$, predictability was considerably enhanced. This modification was applied by assuming that residual compressive stresses were present at the plastic zone in front of the crack tip during each load cycle, thereby negating any environmental contribution to da/dn (growth rate per cycle) until $K_{I\min}$ was exceeded. That this did improve the predictability indicates that the environmental contribution to growth rate is a more complex function of K_I than the model proposed by Wei-Landes, particularly when the $K_{I\min}$ portion of the cyclic load is close to $K_{I\text{scc}}$. Additional work is required to provide a better insight relative to the nature of the exact correction factor.

The activation energy for corrosion fatigue crack growth rate compared more favorably with the 5200 cal/mole activation energy for hydrogen adsorption onto a clean iron surface than for hydrogen diffusion and further supports the conclusion that the failure process is controlled by the hydrogen generating metal environment reaction.

V - REFERENCES

1. R. P. Frohmberg, W. J. Barnett, and A. R. Troiano: Trans. ASM, 1955 Vol. 47, p. 892.

2. A. R. Troiano: Trans. ASM, 1960, Vol. 52, p. 54.

3. N. J. Petch and P. Stables: Nature, Vol, 169, 1952, p. 842.

4. H. H. Johnson, J. G. Moriet, and A. R. Troiano: AIME Trans., Vol. 179, 1957, p. 777.

5. E. A. Steigerwald, F. W. Schaller, and A. R. Troiano: AIME Trans., Vol. 215, 1959, p. 1048.

6. C. F. Barth and E. A. Steigerwald: Met. Trans., Vol. 1, 1970, p. 3451.

7. G. L. Hanna, A. R. Troiano, and E. A. Steigerwald: Trans. ASM, Vol. 57, 1964, p. 658.

8. W. Beck, J. Bockris, J. McBreen, and J. Nanis: Proc. Roy, Soc (London), Vol. A290, 1966, p. 221.

9. H. H. Johnson and A. M. Willner: App. Mat. Res., Vol. 4, 1965, p. 34.

10. C. F. Barth, E. A. Steigerwald, and A. R. Troiano: Corrosion, Vol. 25, No. 9, 1969, p. 353.

11. B. F. Brown, C. T. Fujii, and E. P. Dahlberg: Journal Electrochem. Soc., Vol. 116, 1969, p. 218.

12. C. S. Kortovich and E. A. Steigerwald: Contract N00014-69-C-0286, June 15, 1971, to be published in the Journal of Fracture Mechanics.

13. R. P. Wei, presented at the ASTM/ARPA Symposium on Fundamentals of Stress Corrosion Cracking, Atlanta, Ga., 29 September to 4 October, 1968.

14. H. H. Johnson and A. M. Willner: Applied Materials Research, Vol. 4, 1965, p. 34.

15. G. G. Hancock and H. H. Johnson: Transactions, Metallurgical Soc., Am. Institute Mining, Metallurgical and Petroleum Engrs, April 1966.

16. Che-Yu Li, P. M. Talda and R. P. Wei: International Journal of Fracture Mechanics, Vol. 3, 1967, p. 29.

17. R. P. Wei, P. M. Talda and Che-Yu Li: Fatigue Crack Propagation, ASTM STP 415, Am. Soc. Testing Mats., 1967, p. 460.